[redacted]

STUDY OF INTERACTION OF LOW DOSE POWER SOURCE RADIATION FIELDS WITH SELECTED SPACE SCIENTIFIC INSTRUMENTS

Y-49607

FINAL REPORT

[redacted]

RESEARCH REPORT

BATTELLE NORTHWEST
BATTELLE MEMORIAL INSTITUTE PACIFIC NORTHWEST LABORATORIES
BATTELLE BOULEVARD P. O. BOX 999 RICHLAND, WASHINGTON 99352

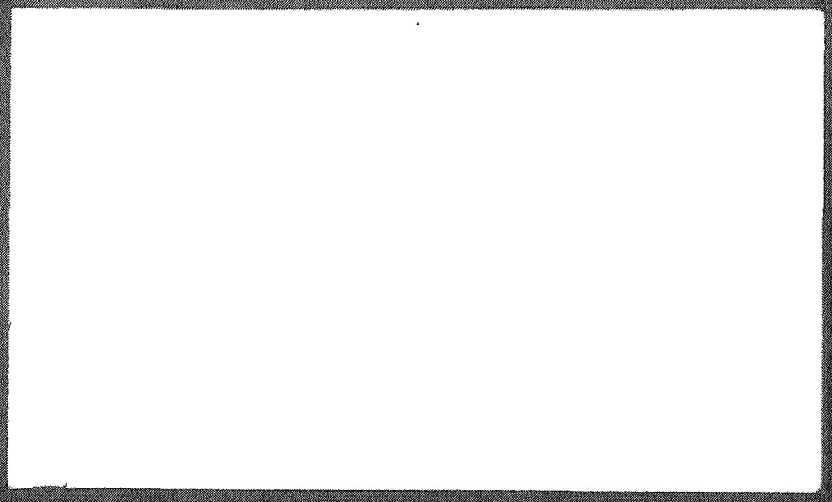

RESEARCH AND DEVELOPMENT CAPABILITIES

Air & Water Pollution
Alloy Development
Analytical Chemistry
Applied Mathematics
Aquatic Biology
Atmospheric Sciences
Biomedical Science & Technology
Biophysics
Catalysis - Surface Chemistry
Cellular & Molecular Biology
Ceramics & Cermets
Chemical Development & Processes
Comparative Pathology & Physiology
Composite Materials
Computer Simulation & Systems Analysis
Computer Technology
Corrosion Technology
Ecology - Radioecology
Electrochemistry
Electromechanical Devices & Systems
Electronic Devices, Circuits & Systems
Energy Conversion Processes
Environmental Sciences
Fluid Mechanics
Food Technology
Geochemistry
Graphite Technology
Heat Transfer
Hydraulics
Hydrology
Industrial & Applied Chemistry
Industrial Economics
Inhalation Toxicology
Inorganic Chemistry
Instrumentation
Laser Technology
Marine Science & Technology
Materials Fabrication
Materials Separation & Purification
Mechanical Components & Devices
Microscopy: X-Ray, Optical & Electron
Mineralogy
Nondestructive Testing
Nuclear Economics
Nuclear Fuels Development, Processing & Separations
Nuclear Instrumentation
Nuclear Physics
Nuclear Reactor Technology
Nuclear Reactor Materials
Nuclear Safeguards Evaluation
Operations Research
Optics
Organic Chemistry
Process & Physical Metallurgy
Physical Chemistry
Plant Nutrition
Process Development
Radiation Biology
Radiation/Irradiation Effects on Materials
Radiation Shielding & Protection
Radioactive Waste Processing & Disposal
Radio & Radiation Chemistry
Radiobiology
Radioisotope Technology & Applications
Radiological Science & Technology
Regional Economics
Seismology
Semiconductors - Solid State Devices
Solid State Physics
Spectroscopy
Statistics
Systems Development & Analysis
Theoretical & Applied Mechanics
Theoretical & Mathematical Physics
Thermodynamics
Toxicology
Ultrasensitive Measurement Methods
Ultrasonics
Water Treatment, Use & Recovery
Welding - Joining Technology

As a research and development organization, the services Battelle offers its sponsors are those beyond the normal scope of the consulting engineering organization. Similarly, Battelle does not contract to perform routine testing of the type offered by commercial testing laboratories. The Battelle concept of research and development is based on its ability to provide the varied scientific and technical skills necessary for the successful solution of a broad array of problems. In addition, Battelle retains a number of consultants to supplement its in-house advisors.

STUDY OF INTERACTION OF LOW DOSE POWER SOURCE RADIATION FIELDS WITH SELECTED SPACE SCIENTIFIC INSTRUMENTS

Y-49607

FINAL REPORT

G. W. R. Endres, R. B. Smith
T. D. Jones and A. J. Haverfield

July 15, 1970

Contract - 952559

Battelle Memorial Institute
Pacific Northwest Laboratories Div.
Post Office Box 999
Richland, Washington 99352

STUDY OF INTERACTION OF GAMMA RAY AND NEUTRON RADIATION WITH SELECTED SPACE SCIENCE INSTRUMENTS

Y-49607

Final Report

G. W. R. Endres, R. B. Smith,
T. D. Jones and A. J. Haverfield

July 15, 1970

Contract - 952559

Battelle Memorial Institute
Pacific Northwest Laboratories Div.
Post Office Box 999
Richland, Washington 99352

This work was performed for the Jet Propulsion Laboratory, California Institute of Technology, as sponsored by the National Aeronautics and Space Administration under Contract NAS7-100.

TECHNICAL CONTENT STATEMENT

This report contains information prepared by Battelle Memorial Institute, Pacific Northwest Laboratories Division, under JPL sub-contract. Its content is not necessarily endorsed by the Jet Propulsion Laboratory, California Institute of Technology, nor the National Aeronautics and Space Administration.

NEW TECHNOLOGY

No reportable items of new technology have been identified.

ABSTRACT

The response of selected surface-barrier and lithium-drifted silicon detectors to photon and neutron radiation is reported. Absorbers of various material were used to shield out primary beta radiation and conversion electrons. For combined detector and absorber, and for energies above a 200 keV bias level, the photon counting efficiency was in the range of 1×10^{-3} to 1×10^{-1} counts per γ per cm^2; depending somewhat on photon energy and detector size.

The neutron counting efficiency could not be unambiguously separated from the photon efficiency due to the impossibility of obtaining γ-free neutron fields. However, an upper limit for the efficiency, about 10^{-2} below that for photons, was obtained over the neutron energy range from 0.20 to 0.73 MeV.

The channel electron multipliers could not be operated without after pulsing and therefore the response measurements could not be conducted.

Response measurements for a type 6213 G-M counter were conducted at photon energies from 0.279 MeV to 2.75 MeV and at neutron energies from 0.20 MeV to 0.73 MeV. Photon response was also measured for lead shielding from 0.01 inches to 0.450 inches thick.

Response measurements for two NE-213 liquid scintillator neutron spectrometers were conducted with monoenergetic neutrons

from 0.73 MeV to 5.0 MeV. Responses were determined for both normal and side incidence of neutrons on the detectors. Response functions were determined as a function of neutron energy for several equivalent electron bias levels from 25 keV to 200 keV.

TABLE OF CONTENTS

Technical Content Statement. i

New Technology ii

Abstract iii

Table of Contents. v

Summary. 1

Introduction 4

I. γ Response of Solid State Detectors. 5

II. Neutron Response of Si Solid State Detectors 15

III. Channel Electron Multiplier - Type CEM-4010. 19

IV. G-M Counter Response Measurements. 21

V. Neutron Spectrometer System. 35

Calibration. 36

Neutron-Gamma Discrimination 37

Neutron Flux Measurements. 38

Data Acquisition 39

Scintillator Response to Protons 40

Treatment of Data. 41

Results. 42

Errors 43

Be(d,n) Thick Target Spectrum. 44

References 46

Appendix A A-1

SUMMARY

This is the Final Report describing the work accomplished on Contract No. 952559 for a "Study of Interaction of Low Dose Power Source Radiation Fields with Selected Space Scientific Instruments." This report is concerned with the measurements taken with the scintillation neutron spectrometer using monoenergetic neutrons, and the measurements taken with silicon surface barrier and lithium drifted detectors, G-M counters and channel electron multipliers using photon and neutron radiation.

The objectives of the work are to determine the radiation responses and the absolute detector efficiency as a function of photon and neutron energy for EON type 6213 Geiger-Muller counters, silicon totally depleted surface barrier detectors, lithium drifted silicon detectors, and type CEM-4010 channeltron* electron multipliers, and to calibrate a scintillation neutron spectrometer and associated electronics supplied by JPL.

This work is being done to provide more precise information about the response of space radiation detectors to radiation fields generated by spacecraft isotopic power sources. The neutron spectrometer is being calibrated to provide spectrum data for monoenergetic neutrons so that measurements of continuous neutron spectra can be made.

---

*Channeltron is a registered trademark of the Bendix Corporation.

Five different thicknesses of silicon surface barrier detectors from 30 microns to 1000 microns were used together with four thicknesses of lithium drifted silicon detectors from about 1 mm to 5 mm drifted depths. Efficiencies for counting photons ranged from about 1×10^{-3} counts per photon per cm^2 for the smallest detector, to about 1×10^{-1} counts per photon per cm^2 for the largest detector at a bias of 200 keV. Measurements were conducted with five photon sources: ^{203}Hg, ^{137}Cs, ^{54}Mn, ^{60}Co and ^{24}Na and two absorbers: 0.220 in Al for ^{24}Na and 0.09 in Al for the other sources. Results were determined for all sources and all detectors except the 30 micron detector which in some cases was so insensitive no counts were obtained above the noise level. The 1 mm and 3 mm lithium drifted detectors yielded inconsistant results in that their efficiencies were not consistant with the stated drift depth.

Neutron measurements were conducted for 0.20, 0.56, and 0.73 MeV monoenergetic neutrons. The resultant efficiencies range from about 1×10^{-5} counts per neutron per cm^2 to about 1×10^{-3} counts per neutron per cm^2 depending on detector thickness. These values are an upper limit to the actual efficiency because of photons present in the neutron beam. In fact, most of the measured response may be due to gamma radiation. The measured "neutron" efficiencies are about two orders of magnitude less than the measured photon efficiencies.

Measurements were conducted with a channel electron multiplier type CEM-4010. Due to a problem with afterpulsing, no confidence can be placed in the counting data, although positive results were obtained for ^{137}Cs, ^{54}Mn, and ^{60}Co sources. The device did not reach the count rate

saturation mode of operation with voltages as high as 4000 volts.

Photon response and shielding experiments were conducted with the 6213 G-M counter. Satisfactory operation was achieved at 550 volts applied to the G-M. Shielding measurements were carried out with 0.010, 0.020, 0.030, 0.050, 0.075, 0.150, 0.300, and 0.450 inches of lead surrounding the side of the G-M counter but no shielding in front of the window. Efficiencies for ^{137}Cs, ^{54}Mn, and ^{60}Co sources agreed well with JPL measurements and manufacturer's specifications for the unshielded counter and side incident photons. Measurements were conducted only for side incidence with the source placed so that photons could not enter the window directly.

The absolute counting efficiency (response) of the two NE-213 scintillators for the fast neutron spectrometer was measured for monoenergetic neutrons from 0.73 to 5.0 MeV at 0.5 MeV intervals. The scintillators were operated in a commercial n,γ discrimination system, and a multichannel analyzer was used to obtain differential pulse height spectra at each neutron energy. The integral response above bias levels from 25 to 200 keV (electron equivalent energy) was obtained by integration of the spectra. Neutron fluence for each run was measured using the Hanford long counter.

For 2 MeV neutrons, and a 50 keV bias level, the response was respectively 1.3 and 2.05 counts per neutron/cm^2 for the 1.5 inch and 2.0 inch diameter scintillators.

Data on the scintillator light output for the recoil protons was also evaluated and found to be consistent with that of other workers.

INTRODUCTION

Since future interplanetary spacecraft will require the use of radioactive isotopic sources to furnish on-board power, the effects of the radiation emitted from the sources on various instrumentation in the spacecraft must be known and evaluated. The purpose of this project is to measure experimentally the response of selected instruments to monoenergetic photon and neutron radiation so proper corrections can be made for the presence of the radiation field internal to the spacecraft. With the energy response of the instruments known, it should be possible to calculate their response to the power source radiation field which is not monoenergetic.

I. γ RESPONSE OF SOLID STATE DETECTORS

The detectors to be investigated consisted of one each of 30μ, 100μ, 300μ, 500μ, and 1000μ thick surface barrier detectors and 1 mm, 2 mm, 3 mm, and 5 mm depletion depth Li drifted silicon detectors. The surface barrier detectors were supplied by Nuclear Diodes, Inc., and the Li drifted detectors by Nuclear Equipment Corporation. The 30μ detector had an area of 0.5 cm^2; all other detectors were 2 cm^2. The isotopic photon sources used and their associated γ energy output were:

^{203}Hg	γ = 0.279 MeV
^{137}Cs	γ = 0.662 MeV
^{54}Mn	γ = 0.835 MeV
^{60}Co	γ_1 = 1.173 MeV
	γ_2 = 1.332 MeV
^{24}Na	γ_1 = 1.369 MeV
	γ_2 = 2.754 MeV

Since all of these sources also emit conversion electrons or beta particlces or both, it was necessary to shield the detector from these particles. Any shielding placed around the detector, however, gives rise to secondary electrons generated by the source γ-rays. To obtain a "pure" photon response by this method is thus impossible to do directly. It is not the pure gamma ray response that is desired since the counters are always surrounded by absorber materials so the effects of secondary electrons generated in this

material must be determined. One can at best try to minimize secondary electron detection interference and interpret as best one can the resulting "impure" response curve. A major problem in all shielding attempts is that some of the detectors approach 100 percent detection efficiency for most of the incident secondary electrons in question, while the γ efficiency varies from a few percent to less than 1 percent, depending on the detector, γ source and bias level.

The γ response was to be determined as the number of integral counts above a series of voltage or corresponding energy bias levels per calculated incident photon flux. It was suggested at first that a simple lower level voltage discriminator and scaler unit be utilized to obtain the results. It was felt, however, that the additional spectral information that could be obtained by use of a multichannel analyzer would be very useful and perhaps necessary. The bias levels of interest correspond to 50 keV, 75 keV, 100 keV, 150 keV and 200 keV of energy deposited in a detector.

The initial experimental set-up was as shown below.

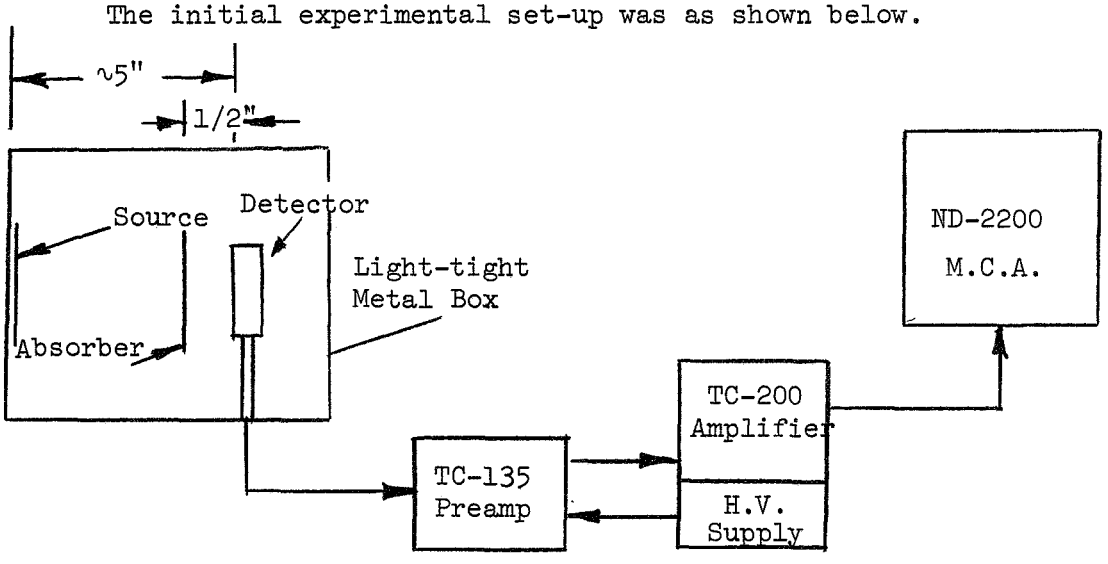

Since the detectors are very sensitive to visible light, they were placed in a light-tight box. This consisted of a metal chassis box approximately 6x8x2 inches, with a cardboard top. The absorbers consisted of 2-1/2x3-1/2 inch sheets of aluminum, graphite, lexan (polycarbonate) or lead placed $\sim$ 1/2 inch in front of the detector. The thickness of each absorber was made as close as possible to the calculated range of an electron in the absorber material with the full energy of the γ-ray being dealt with. It was felt that this thickness would stop the beta or conversion electrons from each source and insure an equilibrium value of escaping secondary electrons which were generated in the absorber. From the empirical formulas, $R = 0.542E - 0.133$ for $0.8 < E < 3$ MeV and $R = 0.407E^{1.38}$ for $0.15 < E < 0.8$ MeV (where R = range in gm/cm^2 and E = energy in MeV),[1] we obtained the following values;

E(MeV)		.279	.662	.835	1.332	2.754
$R(\frac{gm}{cm^2})$		.070	.230	.320	.589	1.493
$R_{aluminum}$	cm	.0259	.0852	.1185	.218	.554
	in	.0102	.0336	.0466	.086	.218
$R_{graphite}$	cm	.0437	.1439	.200	.368	.935
	in	.0172	.0566	.0786	.145	.368
R_{lexan}	cm	.0565	.1855	.2580	.4750	1.204
	in	.0222	.0730	.1020	.187	.475
R_{lead}	cm	.0062	.0203	.0282	.0519	.132
	in	.00242	.0080	.0111	.0204	.052

The charge collected by the detector was fed to a TC-135 charge sensitive preamplifier. The pulse formed here was shaped and further amplified by a TC-200 amplifier. The time constants used were 0.4μ seconds for some detectors and 0.2μ seconds for others. The signal was then stored in 1024 channels of an ND-2200 multichannel analyzer. The leakage current values for the detectors were such that a change in the TC-135 bias resistor was necessitated. It was reduced from 91 x 10^6 ohms to 22 x 10^6 ohms.

Initial runs with the various detectors were made in vacuum. A ^{210}Po α source was used to check resolution. The 1000μ surface barrier detector proved to be too noisy to use and was returned to the vendor, who replaced it with an acceptable one. The 3 mm Li drifted detector later developed excessive noise problems and was repaired by the vendor. The detectors gave measured ^{210}Po α resolutions very close to 30 keV FWHM. Slightly higher FWHM values were obtained for the ^{137}Cs 624 keV conversion electron peak in vacuum.

To calibrate the detector response with energy, it was decided to use a ^{203}Hg source in vacuum. The two conversion peaks, at 194 keV and 264 keV, showed prominently in all but the 30μ detector. Little results were obtained with this detector because of its extremely low sensitivity. The low energy of the ^{203}Hg conversion electrons insures that the peaks should correspond to full energy deposition. Initial calibrations were made to some arbitrary and uneven number in terms of energy per channel. Later, amplifier gain was always adjusted to yield 5 keV per channel, which was most convenient. Results were printed out on paper tape. The tapes

were then totalled or integrated above the channel numbers which corresponded to the five bias energy levels. The linearity of the system was checked periodically by use of a precision pulse generator, which inserted signals into the preamplifier. The results always showed essentially zero linearity deviation from channels 10 through 1024.

The resolution of each detector as measured with the ^{203}Hg source in vacuum is shown in Table 4. Most of the detectors have a full width half maximum (FWHM) resolution of 20 to 30 keV. The 1 mm lithium drifted detector is slightly poorer at 32.5 keV, and the 300, 500, and 1000 micron detectors are slightly better at 18.3 and 17.5 keV.

Background runs were always made with each detector to record both the radiation background and electronic noise contributions to the count rate. Subtraction was then made from the totals for the various bias levels to eliminate these contributions. In a few cases, the lowest bias levels, 50 keV, had such a high noise contribution that it was unreliable.

Initial results are typified in Table 1, which gives the measured response of five detectors at 50 keV bias with the four different absorber materials. First evident was the fact that the type of absorber seemed to make very little difference in the response. In a few of the most extreme cases, the maximum difference in efficiency for the different absorbers is 10 to 15 percent. In most cases, it is much less, being within the uncertainties of the experiment. For the case of ^{54}Mn, which gives the "purest" γ contribution of the sources used, the response for different absorbers is essentially constant. This is especially true for

the lithium drifted detectors, which have a significant dead layer on the back side insensitive to backscattered electrons. Since the absorber thickness in each case is not great enough to cause more than a very few percent γ attenuation, these results might be expected.

All these initial results, however, seemed to indicate somewhat higher responses than were expected. Also, the bare response of some of the detector-source combinations in relation to the absorber-in-place response was higher than expected. These results seemed to indicate excessive background scattering into the detectors.

Three steps were taken to reduce scattering conditions: (1) the metal box was replaced by a larger (10x14x4 inches) cardboard box; (2) the absorber was cut to a circular disc the diameter of the detector; (3) the absorber was moved into virtual contact with the detector. Each of these steps reduced response somewhat. The combined effects decreased responses by a factor of from 10 to 25 percent. The reductions were generally greater, percentage-wise, for the thinner detectors and lower energy sources.

The final experiments were carried out for only the aluminum absorber. Absorber thickness was set at .090 inches for all sources except ^{24}Na, for which it was .220 inches. The increase was necessary for ^{24}Na primarily because of the 2.75 MeV maximum energy gamma present.

The final results are tabulated in Table 2 and shown on Figures 1 through 5. Response is given as the number of counts above a certain bias energy level per calculated incident gamma per square centimeter. The calculated incident gamma value does not take into account any gamma attenuation in the intervening absorb er, which should not be more than a few percent for the worst case.

Several apparent anomalies are noticeable in the figures of the response data. At lower bias levels, the ^{137}Cs response of the surface barrier detectors is apparently high with respect to the responses to sources of neighboring γ energies. It was felt that the relatively high yield 624 keV conversion electrons of ^{137}Cs might be responsible for this by scattering of the cardboard surroundings and entering the back of the detectors. This would not affect the Li drifted detectors because of their metal case backing and back dead layer material. The 300μ surface barrier detector was tested in the experimental set-up, and was found to give 4 to 6 percent less response for ^{137}Cs with a .090 inch circular absorber taped to its back side than with no absorber behind it. Both ^{60}Co and ^{54}Mn gave $\sim$ 5 percent <u>greater</u> response with this absorber behind the detector. This increase in response is due to scattered electrons generated in the rear absorber and should be nearly the same in magnitude for the ^{60}Co as for the ^{54}Mn. Thus, the absorber behind the detector in the ^{137}Cs case must be shielding the detector from an approximately 10 percent contribution to its bare response due to electrons scattered into the back of the detector from the surroundings. These electrons must be largely conversion electrons and not beta particles from the ^{137}Cs because ^{60}Co has a beta spectrum close to that from ^{137}Cs and still shows the increase that ^{54}Mn does, which has no beta component and only an insignificant conversion electron component. Thus, indications are that the true ^{137}Cs response of the surface barrier detectors is less than measured by $\sim$ 10 percent for the 300μ detector.

The largest anomaly is present in the Li drifted detector responses. At all γ energies and bias levels, the 1, 2, and 3 mm detectors exhibit response efficiencies of inverse order to their stated depletion depths. That is, of the three, the "1 mm" detector is most efficient and the "3 mm" detector the least. To investigate this effect, capacitance versus voltage measurements were performed on the detectors. The results are shown in Figures 6 and 7 for the surface barrier and lithium drifted detectors. With increasing voltage, the capacitance decreases as the depletion depth increases. The capacitance values eventually level out to that of the full depletion depth plus stray capacitance. The latter prevent any absolute conclusions about depletion depth, however, for the same types of mounted detectors, capacitance serves for valid comparison of depletion depth. The measured capacitance values occur in the same order as the measured γ efficiencies. Particularly evident is the abnormality of the "3 mm" detector. Both its high capacitance value and its slow change with voltage distinguish it from the others. This strongly suggests that the manufacturer's stated depletion depths are not being obtained for some of the Li drifted detectors. The capacitance measurements cannot be used to determine the actual drift depths in this case because of stay capacity but the relative drift depths should be correct. To further check this possibility, gamma response measurements were made on Battelle-owned detectors of stated drift depths of 2, 3 and 5 mm. Three different 2 mm detectors gave ^{137}Cs gamma responses quantitatively close (similar) to that of our "2 mm" detector. A 5 mm detector gave a gamma response within 10 percent of our "5 mm" detector. A 3 mm detector,

however, gave a response over twice as large as that the JPL "3 mm" detector. Thus, it appears that the JPL "3 mm" detector has a true depletion depth of less than 1 mm, while the JPL "1 mm" detector has a true depletion depth of approximately 3 mm.

Results for the ^{24}Na response (γ_1 = 1.369 MeV, γ_2 = 2.754 MeV) are given both for the total response at the average gamma energy (2.06 MeV) and for the partial response due to the 2.75 MeV component. To do this, subtraction of the 1.37 MeV component from the total response was made by assuming it to be the same as the ^{60}Co response since the differences determined from the response curves were less than 5 percent.

As seen in Figures 1 through 5, the relative efficiency of the different thickness detectors is not constant over the range of gamma-ray energy. That is, the ratio of efficiency between any two detectors is not necessarily constant. With increasing gamma energy, the efficiency of the surface barrier detectors tends to rise, while that of the lithium drifted detectors tends to fall, or to remain constant. The apparent crossing of some of the response curves at high energy is probably not real, the extent of crossing being within the experimental uncertainty. There are at least two factors which might contribute to cause this situation. First, for the thinner surface barrier detectors, as gamma energy increases, an increasing fraction of the response should be due to Compton electrons generated in the absorber. As an example, for ^{24}Na, the 300μ surface barrier detector has almost twenty times its own thickness of aluminum absorber placed in front of it. For the 5 mm Li drifted detector, however, this absorber thickness is roughly equal to the detector thickness. The relative

contribution of the absorber generated Compton electrons to the total measured response is thus much greater for the thin detector than for the thick one. Secondly, there is greater electron scatter into the backs of the surface barrier detectors than into the Li drifted detectors. ^{24}Na has a high energy beta (100 percent yield, 1.39 MeV maximum) which might contribute significantly by this means.

Error limits on the absolute values are indicated on various of the points in Figures 1 through 5. These were assigned on the basis of independent contribution from three sources: statistical error in count rate; source to detector distance measuring error; and source strength uncertainty. Source strength and distance uncertainty each were assigned a value of 3 percent contribution to count rate uncertainty. In some cases, the standard deviation of the count was the dominant uncertainty. In most cases, however, it was equal to or less than the other two factors. The combination of factors gave an uncertainty of 4 to 6 percent for the majority of the data points with a few of the worst cases being as high as 14 to 16 percent. When comparing different biases with the same source, the distance and source strength uncertainties cancel out. When comparing the same detector with different sources, most of the distance uncertainty drops out.

II. NEUTRON RESPONSE OF Si SOLID STATE DETECTORS

Initial attempts were aimed at obtaining neutron responses for six neutron energies between 0.2 MeV and 5 MeV. The neutrons were obtained through T(p,n), C(D,n) and D(D,n) reactions in Battelle's Van de Graaff accelerator. The experimental arrangement was as shown in Figure 8. Protons or deuterons incident on the target material gave rise to a spectrum of neutron energies which are angularly correlated. A long counter[3] was used to monitor flux. It was maintained at a positive angle of 45° to the beam tube and a distance of 100 cm from the target. The detector was placed at a negative angle, θ, to the beam tube such as to be exposed to neutrons of the desired energy from a given reaction. Known parameters relate the long counter count with the flux on the detector for a given distance, angle θ, and target reaction.

It was known that of the three reactions used, only the T(p,n) reaction gives a reasonably small associated gamma-ray yield. It soon became apparent that the various detector responses were at least two orders of magnitude smaller for the neutrons than for gamma-rays of comparable energies. This presents obvious problems of shielding the detectors from the gamma-rays. Efforts were thus concentrated upon obtaining results for neutron energies of 0.20 MeV, 0.56 MeV and 0.73 MeV; all of which were obtainable through the T(p,n) reaction.

The tritium target used for these exposures was thick enough to shift the average energy of the neutrons produced down in energy by 100 to 150 keV. Thus, the results labeled 0.73 MeV are due to neutrons with

an average energy of about 0.60 MeV, which is close to the resonance in the silicon cross section. The results for 0.20 MeV neutrons are an average over the region from 50 keV to 200 keV where the silicon cross section has an anti-resonance.

Initial results showed that even with the T(p,n) reaction, a previously unsuspected high background was contributing to the detector responses. Inverse square runs were made at 4-5 different distances from the target at each of the three energies. The results showed a relatively constant background contribution to the detector responses. At a detector distance of 40 cm from the target, this background term amounts to 30 to 50 percent of the total response of a detector, depending on the particular neutron energy and bias level. The percentage contribution is apparently relatively independent of the particular detector. The source and nature of this background is not adequately known at this time. It is most likely composed of gamma and thermal neutrons scattered in the room. Results obtained are shown in Table 3 and displayed for two bias levels in Figures 9 and 10. For each energy and bias level, background correction was made by subtracting the constant term determined by the inverse square runs made with the 500μ surface barrier detector. Inverse square runs made with a tissue equivalent proportional counter show that the background due to scattered fast neutrons is insignificant. The uncertainty of these results, due to the count statistics of the basic and correctional terms is in the range of 10 to 20 percent for most of the data points. Methods are being proposed to determine both the source and nature of the background contribution, and the fractional contribution of direct target gamma-rays to the responses here reported.

As seen in Figure 9 and 10, there is a definite rise in the response of all the detectors at 0.73 MeV. This is felt to be probably due to the resonance in the silicon neutron cross section just below 0.73 MeV. If this is so, then the reported responses are largely true neutron responses.

The values shown in Figures 9 and 10 result from interpreting all observed counts as neutron events, and dividing by the known neutron flux. These values are roughly two orders of magnitude below the response to similar energy gamma-rays, indicating that the neutron response is at least that small, and perhaps smaller. For such low neutron reqponse, it must be expected that some fraction of the observed counts may be due to gamma-rays (which are unavoidably associated with any neutron fields).

The background which was subtracted off has subsequently been found to be nearly all due to gamma, however, even the inverse square component of the radiation from the target must include some gamma-ray flux. Under these circumstances of low neutron response and non-zero gamma flux, it is not possible to further identify what portion of the observed response is truly due to neutrons. The present values must be used as upper limits to the possible neutron response.

Further work will be necessary to obtain better values for the response or to push the limits lower. Some experiments have been proposed to further identify the components of the inverse square portion of the observed counts. These should shed further light on the nature of the target radiation. Beyond that, it will probably be necessary to resort to time-of-flight techniques.

Until further work is done, the present values are a firm upper limit to the possible neutron response of the silicon detectors.

III. CHANNEL ELECTRON MULTIPLIER - TYPE CEM-4010

The response of the channeltron was to be measured as a function of incident photon energy. Although a considerable amount of effort was spent in attempting to achieve proper operation of this device, that goal was not met. The channeltrons were purchased as specified in a special glass enclosure to facilitate the response measurements. It may be possible that the devices were damaged somehow during the process of enclosing them.

After receiving the channeltrons from the vendor,* they were mounted on a special holder with the necessary resistors in the high voltage circuit. A sharp single pulse was observed directly from the CEM at voltage between 2500 and 2600 volts, far below the saturation voltage. When the voltage was increased, a series of after pulses appeared. The number of after pulses seemed to increase as the high voltage increased and the saturation mode of operation could not be reached. This problem could have been due to outgassing in the sealed glass enclosure, so a vacuum valve and ion gauge were attached to the enclosure to permit positive control of the pressure inside the enclosure.

With the controlled vacuum, noise pulses produced by the CEM were reduced to essentially zero. Positive counting of photons from several sources including ^{60}Co, ^{54}Mn, and ^{24}Na was obtained. Sensitivity of the channeltron at 0.84 MeV, 1.25 MeV and 2.0 MeV (the average of the

---

*Bendix Corporation, Electro-Optics Division.

^{24}Na photons) varied from 1.4×10^{-4} to 2.8×10^{-4} counts per gamma per square centimeter for a high voltage of 3000 volts and shaping time constants in the linear amplifier from 0.4μ's to 3.2μ's. The shaping is necessary to provide proper signals to the multichannel analyzer used. The signals from the CEM still consisted of a pulse train and did not approach saturation operation with the high voltage as high as 4000 volts and the pressure as low as 3×10^{-6} mm Hg. Thus, these particular devices do not seem to operate properly at any attainable voltage and pressure. No confidence can be placed on the data obtained even through the sensitivities measured may be reasonable.

This particular CEM should operate at pressures below 1×10^{-4} mm Hg. Our measurements of the sensitivity were taken at 1×10^{-5} mm Hg. The results for one series of gain measurements taken with a ^{60}Co source are shown in Figure 11. As the voltage is increased, the number of observed events also increases and so also does the gain increase. At 3800 volts, the number of events observed is almost the same as the number of events observed at 4000 volts. From work of Evans[2] saturation should be reached at a voltage of about 3000 volts.

IV. G-M COUNTER RESPONSE MEASUREMENTS

Gamma response and shielding experiments were conducted with the type 6213 geiger tube. Shields of depleted uranium which had been prepared proved to be too radioactive to use. A series of cylindrical Pb shields (2 inches long and varying thicknesses) were made for use instead. Low gamma source activities and the low γ efficiency of the geiger tube necessitated a short source-to-detector distance of $\sim$ 5 cm. Gamma radiation was incident on the detector normal to its cylindrical axis. Background was $\sim$ 1 count/min for the bare detector and decreased as absorber thickness increased.

Response measurements were conducted with the same set of photon sources used for the silicon detector measurements discussed earlier as a function of shielding thickness. Lead thicknesses used were 0.010", 0.020", 0.030", 0.050", 0.075", 0.150", 0.300" and 0.450". These data are summarized in Table 5 for all exposures. The information sheet supplied by the vendor listed the response of the 6213 for ^{137}Cs, ^{54}Mn, and ^{60}Co in the proportion of 1/1.3/1.6. The measurements compare favorably with a relative response ratio of 1/1.3/1.8. These ratios would be expected to be somewhat higher due to the side incidence of the photons. The higher energy photons have a slightly higher probability of penetrating the sides of the G-M tube. The response measurements with ^{137}Cs, ^{54}Mn, and ^{60}Co all show an initial rise as the first section of lead shielding is added then a steady drop as additional shielding is added. This build-up is expected due to secondaries generated in the

lead. The response measurements for both ^{203}Hg and ^{24}Na, on the other hand, show a very sharp drop as the first thickness of lead is added. This indicates the presence of a low energy component which is shielded by the 0.010" and thicker amounts of lead.

A count rate versus high voltage function was experimentally determined and the plateau seemed quite reasonable. An operating voltage of 550 volts as recommended by the manufacturer was chosen as the best point to make further measurements. The plateau is shown in Figure 12, and the shielding measurements in Figure 13.

Measurements of the G-M counter's sensitivity to neutron radiation were made at 0.73 MeV, 0.56 MeV, and 0.20 MeV, the same energies used for the data obtained with the silicon detectors. After correcting for the room background, the sensitivities measured were:

2.2×10^{-5} counts per neutron per cm^2 at 0.73 MeV,
1.4×10^{-5} counts per neutron per cm^2 at 0.56 MeV, and
2.0×10^{-5} counts per neutron per cm^2 at 0.20 MeV.

Statistical uncertainties in these measurements are about $\pm$ 15 percent after making the background correction. The G-M counter data showed a much smaller room background contribution than did the silicon detector data. These measured neutron sensitivities represent an upper limit to the true value because of the gamma contamination of the neutron beam.

In general, the position errors for all the G-M counter measurements should be no more than $\pm$ 2 percent. Counting statistics were $\pm$ 3 percent or less in all cases except where an excessive length of time would be required. The uncertainties in the calibrated sources are quoted by IAEA as 1.0 percent or less except for the ^{137}Cs source which is $\pm$ 1.8 percent.

TABLE 1

γ-RESPONSE - EFFECT OF DIFFERENT ABSORBERS

Old metal box arrangements.
Absorbers 2-1/2" x 3-1/2" placed ∿ 1/2" in front of detector.
Results given for: MrdE 100 @ 53 keV; MrdE 300 @ 50 keV;
MrdE 500 @ 50 keV; NE200-2 @ 52 keV; NE200-5 @ 51 keV.

		Count/γ/cm^2				
Source	Absorber	MrdE 100	MrdE 300	MrdE 500	NE200 2	NE200 5
^{137}Cs	.040" Al	.022	.039	.052	.097	.177
^{137}Cs	.060" C	.021	.041	.050	.094	.176
^{137}Cs	.080" Lexan	.023	.044	.054	.096	.172
^{137}Cs	.009" Pb	.023	.043	.055	.094	.172
^{54}Mn	.046" Al	.009	.025	.036	.088	.166
^{54}Mn	.080" C	.010	.024	.039	.089	.167
^{54}Mn	.110" Lexan	.010	0.23	.041	.089	.167
^{54}Mn	.012" Pb	.010	.023	.038	.087	.166
^{60}Co	.086" Al	.011	.030	.044	.088	.156
^{60}Co	.150" C	.011	.033	.048	.086	.161
^{60}Co	.190" Lexan	.012	.032	.047	.092	.160
^{60}Co	.021" Pb	.010	.027	.041	.084	.154
^{24}Na	.240" Al	.036	.065	.082	.094	.153
^{24}Na	.380" C	.032	.064	.082	.096	.155
^{24}Na	.480" Lex	.035	.068	.085	.093	.154
^{24}Na	.058" Pb	.036	.062	.078	.090	.147

TABLE 2

DETECTOR EFFICIENCY (counts/γ/ cm^2)

Detector	eff_{50}	eff_{75}	eff_{100}	eff_{150}	eff_{200}
^{203}Hg .090" Al					
MrdE 100	.014	.0076	.0039		
MrdE 300	.017	.010	.0064	.0011	.0006
MrdE 500	.032	.020	.012	.0014	.0003
NE200-1	.152	.085	.054	.0076	.0018
NE200-2	.097	.062	.040	.0063	.0014
NE200-3	.048	.030	.020	.0028	.0007
NE200-5	.149	.096	.059	.010	.004
MrdE 1000		.036	.023	.0029	.00053
^{137}Cs .090" Al					
MrdE 100	.019	.013	.0084	.0034	.0015
MrdE 300	.021	.017	.014	.0094	.0063
MrdE 500	.038	.030	.023	.0160	.0114
NE200-1	.122	.107	.093	.074	.060
NE200-2	.091	.078	.068	.054	.044
NE200-3	.048	.040	.035	.027	.022
NE200-5	.154	.133	.116	.092	.067
MrdE 1000		.051	.041	.029	.022
^{54}Mn .090" Al					
MrdE 100	.012	.0091	.0063	.0023	.0013
MrdE 300	.020	.015	.012	.010	.0071
MrdE 500	.030	.025	.021	.016	.012
NE200-1		.110	.096	.079	.068
NE200-2	.089	.078	.070	.059	.050
NE200-3	.052	.044	.039	.032	.026
NE200-5	.152	.134	.120	.099	.082
MrdE 1000		.049	.043	.033	.028

- continued -

TABLE 2 (cont'd)

Detector	eff_{50}	eff_{75}	eff_{100}	eff_{150}	eff_{200}
^{60}Co .090" Al					
MrdE 100	.015	.010	.0069	.0035	.0019
MrdE 300	.024	.020	.017	.012	.009
MrdE 500	.038	.032	.028	.021	.017
NE200-1		.104	.094	.082	.073
NE200-2	.008	.079	.072	.062	.056
NE200-3	.052	.047	.043	.037	.032
NE200-5	.142	.131	.121	.106	.093
MrdE 1000		.053	.048	.039	.033
^{24}Na $E\gamma$ = 2.75 MeV .220" Al					
MrdE 30	.0				
MrdE 100	.028	.017	.011	.0054	.0020
MrdE 300	.066	.059	.047	.028	.020
MrdE 500	.085	.072	.063	.049	.034
MrdE 1000		.081	.074	.063	.055
NE200-1		.077	.076	.072	.067
NE200-2	.076	.074	.072	.069	.064
NE200-3	.056	.054	.053	.049	.046
NE200-4	.122	.116	.112	.106	.101
^{24}Na $E_{\gamma average}$ = 2.06 MeV					
MrdE	.0043	.0024	.0011	.0003	
MrdE 100	.021	.013	.009	.004	.002
MrdE 300	.045	.039	.032	.019	.013
MrdE 500	.061	.052	.045	.035	.025
MrdE 1000		.066	.060	.050	.043
NE200-1	.097	.090	.085	.077	.070
NE200-2	.082	.076	.072	.065	.060
NE200-3	.054	.051	.048	.043	.039
NE200-5	.132	.124	.117	.107	.097

TABLE 3

Si SOLID STATE DETECTORS - NEUTRON RESPONSE

BKGD subtracted on basis of constant term arrived at from inverse square runs.

L.C. @ + 45°, 100 cm: Detectors @ - 45°, 40 cm.

		Counts/n/cm^2 x 10^4				
Detector	$E_{neutron}$	200 keV Bias	150 keV Bias	100 keV Bias	75 keV Bias	50 keV Bias
MrdE 100	0.20 MeV		0.09	0.52	0.81	
MrdE 300	0.20 MeV	0.52	0.88	1.76	2.52	3.15
MrdE 500	0.20 MeV	1.15	1.95	3.68	3.78	4.98
MrdE 1000	0.20 MeV	3.93	4.66	5.90	6.02	6.29
NE200-1	0.20 MeV	5.36	6.26	7.80	8.01	8.30
NE200-2	0.20 MeV	4.81	5.61	7.04	7.21	7.47
NE200-3	0.20 MeV	4.30	4.90	5.85	5.65	5.56
NE200-5	0.20 MeV	6.62	7.86	10.04	10.53	
MrdE 100	0.56 MeV	0.07	0.17	0.42	0.66	
MrdE 300	0.56 MeV	0.50	0.86	1.53	2.32	3.24
MrdE 500	0.56 MeV	0.67	1.31	2.82	3.25	3.63
MrdE 1000	0.56 MeV	3.60	4.35	5.17	5.82	6.96
NE200-1	0.56 MeV	4.94	5.85	6.88	7.81	9.73
NE200-2	0.56 MeV	4.59	5.38	6.17	6.92	8.47
NE200-3	0.56 MeV	3.51	4.06	4.52	4.89	5.67
NE200-5	0.56 MeV	6.15	7.34	8.69	9.99	
MrdE 100	0.73 MeV	0.11	0.23	0.55	1.00	
MrdE 300	0.73 MeV	0.57	0.99	1.89	3.28	4.52
MrdE 500	0.73 MeV	1.51	2.55	4.69	5.26	6.12
MrdE 1000	0.73 MeV	4.19	5.07	6.49	8.30	11.18
NE200-1	0.73 MeV	5.59	6.66	8.27	10.68	15.59
NE200-2	0.73 MeV	4.95	5.87	7.27	11.28	
NE200-3	0.73 MeV	4.09	4.72	5.56	6.88	9.06
NE200-5	0.73 MeV	6.82	8.17	10.39	13.80	

TABLE 4

DETECTOR RESOLUTION

Detector Number	Resolution (FWHM)
MrdE 30	24.0 keV
MrdE 100	22.0 keV
MrdE 300	18.2 keV
MrdE 500	18.3 keV
MrdE 1000	17.5 keV
NE 200-1	32.5 keV
NE 200-2	30.0 keV
NE 200-3	28.4 keV
NE 200-5	21.3 keV

TABLE 5

G-M COUNTER RESPONSE VS. Pb SHIELDING

Pb Thickness (in)	^{203}Hg (cts/γ/cm^2)	^{137}Cs (cts/γ/cm^2)	^{54}Mn (cts/γ/cm^2)	^{60}Co (cts/γ/cm^2)	^{24}Na (ave) (cts/γ/cm^2)	^{24}Na (2.75 MeV) (cts/γ/cm^2)
0	5.5×10^{-4}	6.2×10^{-4}	7.9×10^{-4}	11.4×10^{-4}	23.7×10^{-4}	35.9×10^{-4}
0.010	4.5×10^{-4}	6.5×10^{-4}	8.3×10^{-4}	12.3×10^{-4}	20.6×10^{-4}	29.0×10^{-4}
0.020	3.6×10^{-4}	6.4×10^{-4}	8.4×10^{-4}	12.2×10^{-4}	20.3×10^{-4}	28.4×10^{-4}
0.030		5.9×10^{-4}	7.9×10^{-4}		20.5×10^{-4}	
0.050	2.4×10^{-4}	5.7×10^{-4}	7.6×10^{-4}	12.0×10^{-4}	19.6×10^{-4}	27.2×10^{-4}
0.075	1.75×10^{-4}	5.6×10^{-4}	7.3×10^{-4}	12.3×10^{-4}	18.7×10^{-4}	25.1×10^{-4}
0.150	0.67×10^{-4}	4.2×10^{-4}	6.7×10^{-4}	11.3×10^{-4}	17.8×10^{-4}	
0.300		3.2×10^{-4}	4.7×10^{-4}	9.2×10^{-4}	15.6×10^{-4}	22.1×10^{-4}
0.450		2.2×10^{-4}	3.8×10^{-4}	8.2×10^{-4}	13.4×10^{-4}	18.5×10^{-4}

TABLE 6

SYSTEM PARAMETERS FOR SCINTILLATOR RUNS

Neutron Energy	Target Reaction	Incident Energy Ep or Ed	Angular-Position		Gain Setting (DDL Amp)	Resolution[6] and Lowest Bias E_B[7]			
			[4] Scintillator	[5] Monitor (Long Counter)		1.5" Diam		2" Diam	
						ΔE	E_B	ΔE	E_B
MeV		MeV	deg.	deg.		keV/Ch	keV	keV/Ch	keV
0.733	[1] T(p,n)	1.8	45	45	x 32	3.3	25	4.05	30.4
1.00	T(p,n)	1.8	0	45	x 32	3.3	25	4.05	30.4
1.48	[2] C^{12}(d,n)	1.8	0	45	x 32	3.3	25	4.05	30.4
2.00	[3] D(d,n)	1.0	135	135	x 32	3.3	25	4.05	30.4
2.49	D D(d,n)	1.6	105	105	x 32	3.3	25	4.05	30.4
2.99	D(d,n)	0.5	75	75	x 16	6.7	50	8.1	60.8
3.50	D(d,n)	0.8	45	45	x 16	6.7	50	8.1	60.8
3.91	D(d,n)	1.3	45	45	x 8	13.3	100	16.2	121
3.99	D(d,n)	1.4	45	45	x 16	6.7	50	8.1	60.8
4.50	D(d,n)	1.3	0	45	x 8	13.3	100	16.2	121
5.04	D(d,n)	1.8	0	45	x 8	13.3	100	16.2	121

[1] Tritium: in Titanium (T/Ti = 0.52), 476 μgm/cm^2 on platinum disc.

[2] Carbon-12: 603 μgm/cm^2 on tantalum disc.

[3] Deuterium: in titanium (D/Ti = 1.17), 1106 μgm/cm^2 on plantinum disc.

[4] The distance from target to center of scintillator was 75 ± 0.2 centimeters for all runs.

[5] The distance from target to long counter reference plane was 89.7 ± .2 centimeters for all runs. Effective center of counter is behind the reference plane approximately 10 cm, but is a function of energy.

[6] All spectra were accumulated in 256 channel groups.

[7] E_B is the effective bias level in the n,γ discriminating system. Integrated response for bias levels below E_B cannot be obtained.

TABLE 7

INTEGRAL RESPONSE OF SCINTILLATOR

(2.0" Diam. x 0.4" thick, normal incidence, projected area = 20.3 cm^2. Counts above bias level per unit fluence (neut/cm^2).

Bias Level (keV electron equivalent)	Threshold E_n (MeV)	0.733	1.00	1.48	2.00	2.49	2.99	3.50	3.91	3.99	5.04
25	0.24										
50	0.40	1.91	2.50	2.09	2.02	2.00					
75	0.54	1.07	1.94	1.87	1.86	1.82	1.74	1.70		1.60	
100	0.65	0.38	1.37	1.66	1.71	1.65	1.65	1.63		1.51	
125	0.74	0.04	0.85	1.45	1.57	1.50	1.56	1.55	1.34	1.43	1.12
150	0.84	0.00	0.45	1.25	1.45	1.37	1.48	1.49	1.30	1.35	1.10
175	0.92	0.00	0.165	1.06	1.33	1.27	1.40	1.42	1.29	1.26	1.08
200	1.0	0.00	0.024	0.88	1.23	1.18	1.33	1.36	1.21	1.23	1.05

TABLE 8

INTEGRAL RESPONSE OF SCINTILLATOR

(2.0" Diam x 0.4" thick, side incidence, projected area 5.16 cm^2. Counts above bias level, per unit fluence (neut/cm^2)

Bias Level (keV electron equivalent)	Threshold E_n (MeV)	E_n - Neutron Energy (MeV)									
		0.733	1.00	1.48	2.00	2.49	2.99	3.50	3.91	3.99	5.04
25	0.24										
50	0.40	1.25	1.69	1.69	1.55	1.56					
75	0.54	0.65	1.31	1.52	1.42	1.43	1.36	1.34		1.30	
100	0.65	0.09	0.93	1.34	1.31	1.30	1.29	1.28		1.24	
125	0.74	0.02	0.57	1.17	1.21	1.19	1.22	1.23	1.06	1.17	0.96
150	0.84	0.00	0.29	1.01	1.11	1.10	1.16	1.17	1.03	1.11	0.95
175	0.92	0.00	0.103	0.85	1.03	1.02	1.10	1.12	1.00	1.06	0.92
200	1.0	0.00	0.014	0.69	0.94	0.96	1.05	1.08	1.02	0.97	0.90

TABLE 9

MEASURED INTEGRAL RESPONSE OF SCINTILLATOR

(1.5" Diam x 0.4" thick, normal incidence, projected area 11.4 cm^2. Counts above bias level, per unit fluence (neut/cm^2)

Bias Level (keV electron equivalent)	Threshold E_n (MeV)	E_n - Neutron Energy (MeV)									
		0.733	1.00	1.48	2.00	2.49	2.99	3.50	3.99	4.50	5.04
25	0.24	1.84	2.00	1.79	1.47	1.48					
50	0.40	1.31	1.65	1.62	1.31	1.35	1.21	1.21	1.14		
75	0.54	0.74	1.27	1.45	1.19	1.21	1.14	1.16	1.07		
100	0.65	0.28	0.92	1.27	1.09	1.09	1.07	1.10	1.00	0.88	0.82
125	0.74	0.035	0.60	1.10	1.00	0.99	1.01	1.05	0.95	0.85	0.79
150	0.84	0.00	0.35	0.96	0.93	0.91	0.96	1.01	0.90	0.83	0.77
175	0.92	0.00	0.146	0.82	0.86	0.84	0.91	0.96	0.86	0.80	0.75
200	1.00	0.00	0.024	0.68	0.79	0.78	0.86	0.93	0.83	0.78	0.72

TABLE 10

MEASURED INTEGRAL RESPONSE OF SCINTILLATOR

(1.5" diam x 0.4" thick, side incidence, projected area = 3.87 cm^2
Counts above bias level, per unit fluence (neut/cm^2)

Bias Level (keV Electron Equivalent)	Threshold E_n (MeV)	E_n - Neutron Energy (MeV)									
		0.733	1.00	1.48	2.00	2.49	2.99	3.50	3.99	4.50	5.04
25	0.24	1.29	1.37		1.17	1.15					
50	0.40	0.90	1.13	1.33	1.05	1.06	0.99	0.96	0.92		
75	0.54	0.48	0.88	1.20	0.96	0.97	0.94	0.92	0.87		
100	0.65	0.157	0.63	1.05	0.88	0.89	0.88	0.88	0.82	0.74	0.71
125	0.74	0.015	0.41	0.91	0.81	0.81	0.83	0.83	0.77	0.72	0.69
150	0.84	0.00	0.230	0.79	0.75	0.75	0.79	0.80	0.74	0.70	0.67
175	0.92	0.00	0.093	0.67	0.69	0.70	0.75	0.76	0.70	0.68	0.65
200	1.00	0.00	0.015	0.55	0.63	0.65	0.71	0.73	0.68	0.66	0.64

V. NEUTRON SPECTROMETER SYSTEM

The scintillation neutron spectrometer system was supplied by JPL with the exception of some additional components such as DDL amplifier, multichannel analyzer, printer, and a plotter which were BNW supplied. The main components were ORTEC equipment, and they were connected and operated according to the manufacturer's block diagram. The appendix contains a block diagram of the complete system, together with the control settings as used for these measurements.

Two scintillators were measured; one was 2.0 inch diameter by 0.4 inch thick NE-213 in one of the manufacturer's standard cells. The other was 1.5 inch diameter by 0.4 inch thick. For our own purposes, these were sometimes identified as JPL No. 1 and JPL No. 2, respectively. Each scintillator was mounted in turn on the same P.M. tube.

The 2-inch diameter scintillator contained a small bubble a few mm in diameter. Although undesirable, this bubble could not be eliminated, but it was believed to cause negligible effect on the measurements.

The scintillator-P.M. tube assembly was always operated with its axis horizontal, which meant that the circular plane of the scintillator was vertical. Measurements were made with neutrons incident both along the axis (normally to the plane of the scintillator) and perpendicular to the axis (incident on the cylindrical side of the scintillator).

The measurements were carried out with the geometry shown in Figure 8. Table 6 lists the operating parameters for the various runs.

Shown are the neutron energy, target reaction and incident particle energy used, the position of detector and neutron flux monitor, and the gain settings with the resultant pulse height resolution with which the data was acquired.

Calibration

The pulse height scale for the system was calibrated by means of the Compton-edge electrons from the cesium-137 γ-ray (E_γ = 661.6 keV, E_c = 477.3 keV). Following Flynn[4] and Moore[5], the point at the half height of the ^{137}Cs spectra was assigned a value of E_c x 1.04, or 496.4 keV.

The linearity and channel zero setting were checked by means of a precision pulser, and both were always within one channel of the 256 channel group size used. The pulser was connected to the amplifier in place of the linear output from the P.M. tube base, and thus only the linearity of the amplifier and multichannel analyzer was checked. Linearity of the P.M. tube gain and tube base preamp was presumed from the integrity of the manufacturer.

The calibration factor (keV/channel) for the two scintillators was not equal. Primarily this is believed due to different light collection efficiency (the 2-inch diameter scintillator had a glass window larger than the photocathode of the P.M. tube). However, the two scintillators were manufactured at different times, and there is possibly some additional difference in the scintillator material. There is also a difference in resolution for the two scintillators. For the 2-inch diameter scintillator, the resolution was 14 to 15 percent, and for the 1.5-inch diameter about 12 percent. As may be inferred from the last columns of

Table 6, the light efficiency for the 2-inch diameter scintillator is about 18 percent less than that of the 1.5-inch diameter.

The pulse height scale used here is expressed in units of keV electrons equivalent. It is a truly linear scale, even though the response of scintillators to electrons may be somewhat non-linear.[4,6] Linearity with respect to light output is assured by the nature of the system. Calibration in terms of light output from electrons at one energy provides a convenient scale which is independent of light collection efficiency. When comparisons are made of data obtained by different workers (using scales calibrated by different electron energies) some care should be taken to assure equivalence of pulse height scales. For a large body of work done at ORNL, Verbinskii and coworkers[7,8] used a scale of "light units" based on the ^{22}Na γ-spectrum. That unit is closely equivalent to the output from a 1.24 MeV electron.

A typical ^{137}Cs calibration spectrum is shown in Figure 14.

There were slight differences in the calibration factor obtained at different times during the period of the run. However, since these differences were less than 2 percent in all cases, a single set of average calibration factors (consistent with the x 2 changes in gain) was used to give the energy scale for the runs.

Neutron-Gamma Discrimination

Operation of a liquid scintillator fast neutron spectrometer system is entirely dependent on clear n,γ discrimination. No significant

number of γ's should be counted nor, similarly, few neutrons not counted. Operating such a system introduces some practical problems in making these measurements. First, the timing adjustments which make the n,γ discrimination possible are critical, and need to be checked and adjusted frequently. It was, for example, necessary to use slightly different timing settings at each of the amplifier gain settings. Second, it is not possible to achieve good n,γ discrimination at the lowest pulse heights - below about 1/32 of full scale (some other systems claim a 50:1 dynamic range).

Figure 15 shows some typical n,γ timing spectra. The important adjustment is the setting of the timing discriminator relative to the two peaks, within nanoseconds, say.

Estimation of the amount of "tail" of each peak falling beyond the discriminator setting provides some measure of the number of neutrons missed or gammas incorrectly counted. Here, this amounts to, at most, a few percent. Checks with the ^{137}Cs spectra showed that as few as one count in 10^3 would be accepted as neutrons. For any lower setting of the pulse amplitude discriminator, much worse resolution between neutrons and gamma events resulted.

Neutron Flux Measurement

The integrated neutron flux (fluence) during each run was monitored by the long counter.[3] Whenever possible, it and the scintillator detector were positioned symmetrically with respect to the beam tube. This was assumed to provide equal flux at both. Where symmetry was not possible, a correction for the angular variation of the neutron intensity was necessary.

The stability of the long counter efficiency was checked daily by means of a PuBe source inserted in the standard position in the counter.

The neutron fluence was calculated from the following equation:

$$F = N_M \cdot \left(\frac{r_m}{r_s}\right)^2 \cdot \frac{60}{\eta(E) \cdot S_o} \cdot R_\theta \qquad (\text{neutrons/cm}^2)$$

$F(\text{neut/cm}^2)$ is the time integrated fluence at the scintillator.

N_M (counts) is the total counts (during a run) from the long counter.

r_M (cm) is the distance to the effective center of the long counter

$$r_M = 89.7 + 7.8 + 1.1 \cdot E_n \text{ (MeV) cm}$$

r_s (cm) is the distance to the scintillator.

$\eta(E)(-)$ is the efficiency of the long counter as a function of energy (Reference 3, Figure 13).

S_o [(counts/min)/neut/cm^2·sec] is the sensitivity factor for the particular BF_3 tube used in the long counter. $S_o = 209$ (the factor 60 converts from cts/min to cts/sec).

$R_\theta(-)$ is an angular correction factor which differs from unity only when the scintillator and long counter were not symmetrically positioned. Measured values were used.

Data Acquisition

All the data were recorded as differential pulse height spectra. At each neutron energy and scintillator orientation, spectra were accumulated for a preset number of monitor counts. Each spectrum was printed

out in digital form as well as plotted (usually on a logarithmic scale) by a fast plotter.

Occasionally between neutron runs, ^{137}Cs spectra were taken to verify gain calibration; and the timing spectrum using a PuBe neutron source was also taken to check on the settings of the n,γ discrimination. The discriminator setting, separating the n,γ events, was the most critical since gain changes and warm-up caused changes in the timing spectra.

Some typical spectra are shown in Figure 16, and the spectra from all runs are available.

Scintillator Response to Protons

The light output of NE-213 as a function of charged particle energy has been extensively studied before. Such information, for protons, is inherent in the present data; and it is worth considering as a check on internal consistency of the data for the two scintillators as well as with earlier work.

The pulse height vs. maximum proton recoil energy is shown in Figure 17. The data points are from the present data based on an arbitrary definition of maximum pulse height. Because the present spectra have essentially no plateau, a half-height-edge to the spectra is impossible to define well. Instead, the end point of each spectra is used - defined as the channel at which the spectra drops to 1/100 of the level it has at about one/half the maximum channel. Define this way, the maximum pulse height may be expected to be higher than from other definitions due to resolution smearing.

The data points shown in Figure 17 include all runs for both scintillators and both orientations. Agreement at each energy is quite good, indicating a consistent pulse height scale for both scintillators, in spite of their differences in light efficiency. A power law curve, E^{γ}, has been fitted to the data points, and is shown. The best fitting exponent was $\gamma = 1.45$, compared to a 1.5 which some workers have indicated to be a good approximation for this range of proton energy.

Verbinskii and coworkers at ORNL have used a "light table" for protons which has good internal consistency (2 percent) within their Monte Carlo calculations and experiments. Converted from their "light unit" scale to electron equivalent energy, their curve is also plotted in Figure 17. The present data falls 5 to 10 percent above the ORNL curve - which is about what one would expect from the present definition of pulse height and the 12 to 14 percent resolution. Thus, the light scale here used is consistent with other measurements and supports the accuracy of the assignment of the bias levels.

Treatment of the Data

The differential pulse height spectra for all runs were punched into cards and used for input to a simple computer program which integrated each above the several selected bias levels. The channels at which to start the integration were calculated from the resolution (keV/channel) for each run as listed in Table 6. Interpolation to 1/10 of a channel was made. That is, if the calculated bias level fell within a channel,

an appropriate fraction of the counts within that channel was included in the integration.

The integrated counts for each bias level and run were divided by the appropriate value of fluence for the run to convert each to an efficiency value.

Results

The measured response as a function of neutrons energy is shown in Figures 18 through 21 for both scintillators, and for neutrons incident both from the side and normal to the circular plane of the detector. The same data are also listed in Tables 7 through 10.

The response is given as total counts (above the respective bias levels) per unit fluence. On the right side of the graphs is a scale obtained by dividing the response values by the projected area of the detector - that is, counts per cm^2 of detector area. This is entirely equivalent to the scale of counts per single neutron incident on the whole detector - which has been frequently used in calculations of detector efficiency.[7,8,9]

Results are not available at the higher neutron energies for the lowest bias levels. The differential spectra do not extend to these bias levels because of the necessary amplitude discriminator in the n,γ discrimination system.

The points at which the curves intercept the zero response axis (below E_n = 1.0 MeV) are obtained directly from the curve of Figure 17 -

the end points of the differential spectra. For neutrons of energy below these values no pulses would be expected to fall above the respective bias levels. These are listed as the E_n threshold in Tables 7 through 10. (They are the same for all four figures and tables.)

For the 2-inch diameter scintillator, Figures 18 and 19, the point at E_n = 3.91 MeV introduces a jog in the response curve. The lines are drawn through these points only to make clear with which curve they are associated. It shouldn't be implied that there is any fluctuation in response at this energy. The difference between the set of points at 3.91 and 3.99 MeV provides one indication of the consistency of measurements made at somewhat different combinations of deuteron beam energy and laboratory angle. The difference in this case is about 3 percent. (The point at 3.91 was actually intended to be for 4.5 MeV, but the detector was inadvertently positioned at the wrong angle of 45" instead of 0°.)

Errors

The greatest source of uncertainty in the neutron flux arises in the values for efficiency of the long counter - primarily its variation with energy. The absolute counting efficiency of the counter has been measured using the U.S. standard neutron source, NBS-II. The maximum variation in efficiency over the 1-5 MeV range is ± 10 so errors would be very unlikely to exceed that amount. Comparisons of fluence measured by the long counter and a completely independent method, the proton recoil proportional counter, have recently been showing agreement within ± 5 to 10

percent. Therefore, though the measurement may be better than 10 percent, we believe that figure is appropriate.

The stability and reproducibility of the long counter is quite good. The count rate from the inserted PuBe source has been stable within < 1 percent for the last five years. (That is, it follows the predicted growth rate of the source: 1.08 percent/year.) Thus, comparisons between runs made at the same energy should be valid to less than a few percent.

Uncertainties due to counting statistics are negligible in all cases since 10^5 to 10^6 counts were accumulated from the monitor, and 10^4 to 10^6 counts from the scintillator for all runs.

Be(d,n) Thick Target Spectrum

Early in this contract, some irradiations of gyros and oils were performed for JPL using the BE(d,n) reaction with E_d = 1.8 MeV. A time-of-flight spectrum was later taken in order to characterize the energy spectrum of that flux, and, in particular, to obtain a figure for the average neutron energy.

For a detector, the 2-inch diameter NE0213 scintillator was used with normal incidence, and at a 68 cm flight distance. No n,γ discrimination was used since most γ-counts are separated in time from any neutrons, and they provide a convenient reference point for time zero. Under this condition, the only discriminator in the system was that in the ORTEC P.M. tube base and it was set to just reject tube noise. Neutron pulses were

accepted which were considerably lower than any bias level used during the response measurements.

In reducing the time-of-flight spectrum to an energy spectrum, it is necessary to factor in the variation with energy of both the channel width and scintillator response. For the latter, a calculated response of the scintillator, supplied by JPL, was used. The particular curve used was for the 1.016 cm thickness, and for a 10 keV bias. The latter value was chosen because it was the lowest one of the set provided, and most closely corresponded to the scintillator bias situation just described. Our measured scintillator responses were not used because they did not extend to these low bias values.

A small FOCAL program was written for the PDP-8 to perform the required calculations for background subtraction, flight-time to energy conversion, conversion of counts to neutrons using manually entered values of detector response, and finally calculation of average energy.

Figure 22 shows the final neutron spectrum and the value of the average energy, 2.76 MeV. (In monthly reports, some previous values of the average energy were reported for this data. Firstly, a rough value of 3.33 MeV was obtained using only the hydrogen cross section. Secondly, the plot of calculated response for the scintillator, informally supplied by JPL, was used and yielded a value of 2.86 MeV. However, the unlabled energy scale of the plot was incorrectly interpreted to be 0-10 MeV rather than 0-20 MeV. The present value of 2.76 MeV for the average energy was obtained using the correct scale of 0-20 MeV and it supercedes the values previously reported.)

REFERENCES

1. C. M. H. Smith, Nuclear Physics, p. 426, Pergamon Press, New Yor,1966.

2. D. S. Evans, "Low Energy Charged Particle Detection Using the Continuous Channel Electron Multiplier," Review of Scientific Instruments, Vol. 36, No. 3., March 1965.

3. J. DePangher and L. L. Nichols, "A Precision Long Counter for Measuring Fast Neutron Flux," BNWL-260, June 1966.

4. K. F. Flynn, et al., "Pulse Height-Energy Relations for Electrons and Alpha Particles in a Liquid Scintillator," Nuclear Instruments and Methods, 27, p. 13-17, 1964.

5. J. G. Moore and K. F. Orton, "The Interpretation of Pulse Height Distributions in Organic Phosphors," in Selected Topics in Radiation Dosimetry, p. 227-235, IAEA Proceedings Series, 1961

6. D. L. Smith, R. G. Polk, and T. G. Miller, "Measurement of the Response of Several Organic Scintillators to Electrons, Protons, and Deuterons," Nuclear Instruments and Methods, 64, p. 157-166, 1968.

7. V. V. Verbinskii, "Calibration of an Organic Scintillator for Neutron Spectrometry," Nuclear Instruments and Methods, 65, p. 8-25, 1968. Also, ORNL-TM-2183.

8. R. E. Textor and V. V. Verbinskii, "05S: A Monte Carlo Code for Calculating Pulse Height Distributions due to Monoenergetic Neutrons Incident on Organic Scintillators," ORNL-4160, February, 1968.

9. A. A. O'Dell, C. W. Sandifer, and T. B Knowlen, "Neutron Counting Efficiency and Charged Particle Response of an NE-213 Flux Detector," EGG-1183-2172, January, 1968.

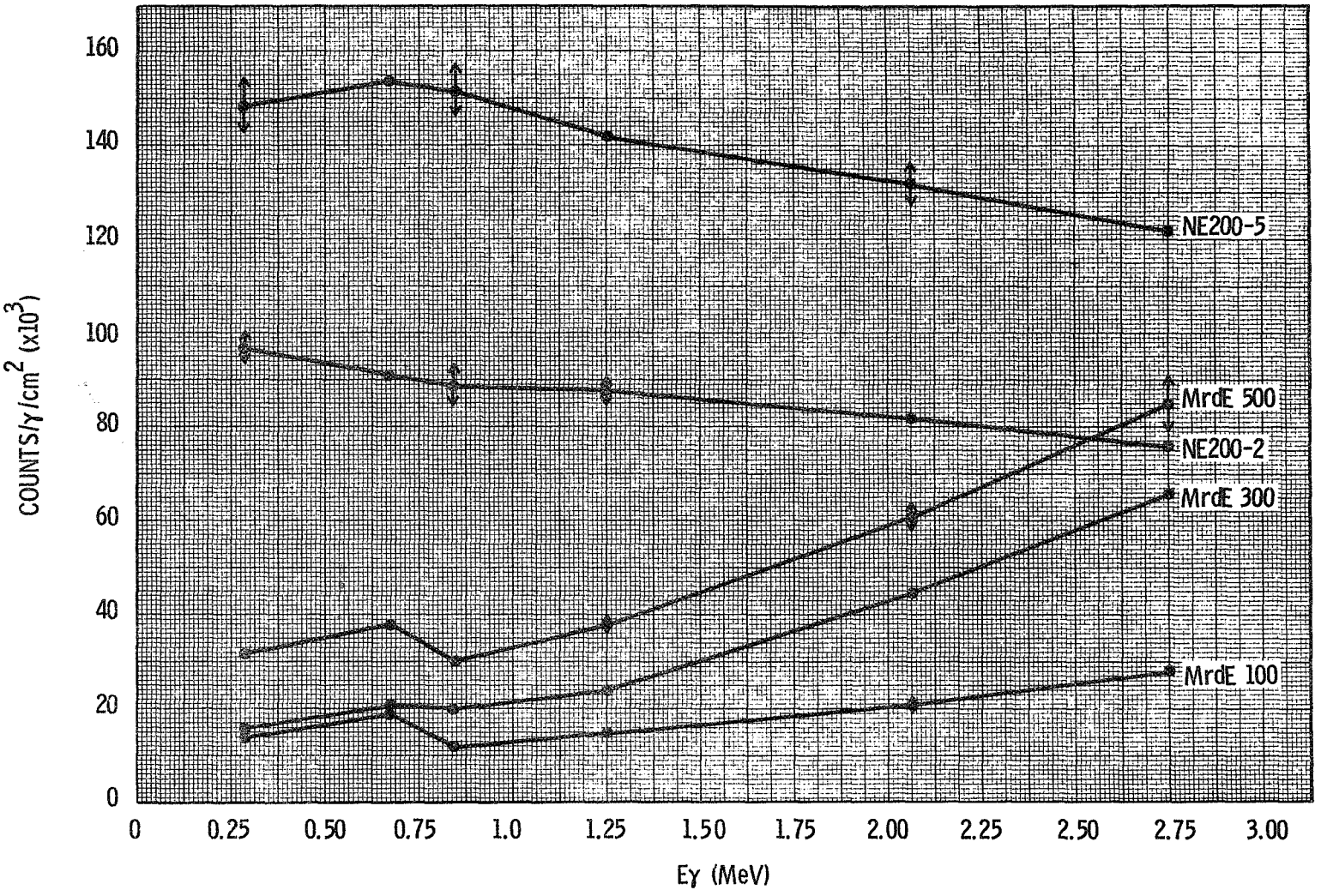

FIGURE 1. DETECTOR RESPONSE VS γENERGY - 50 keV BIAS LEVEL

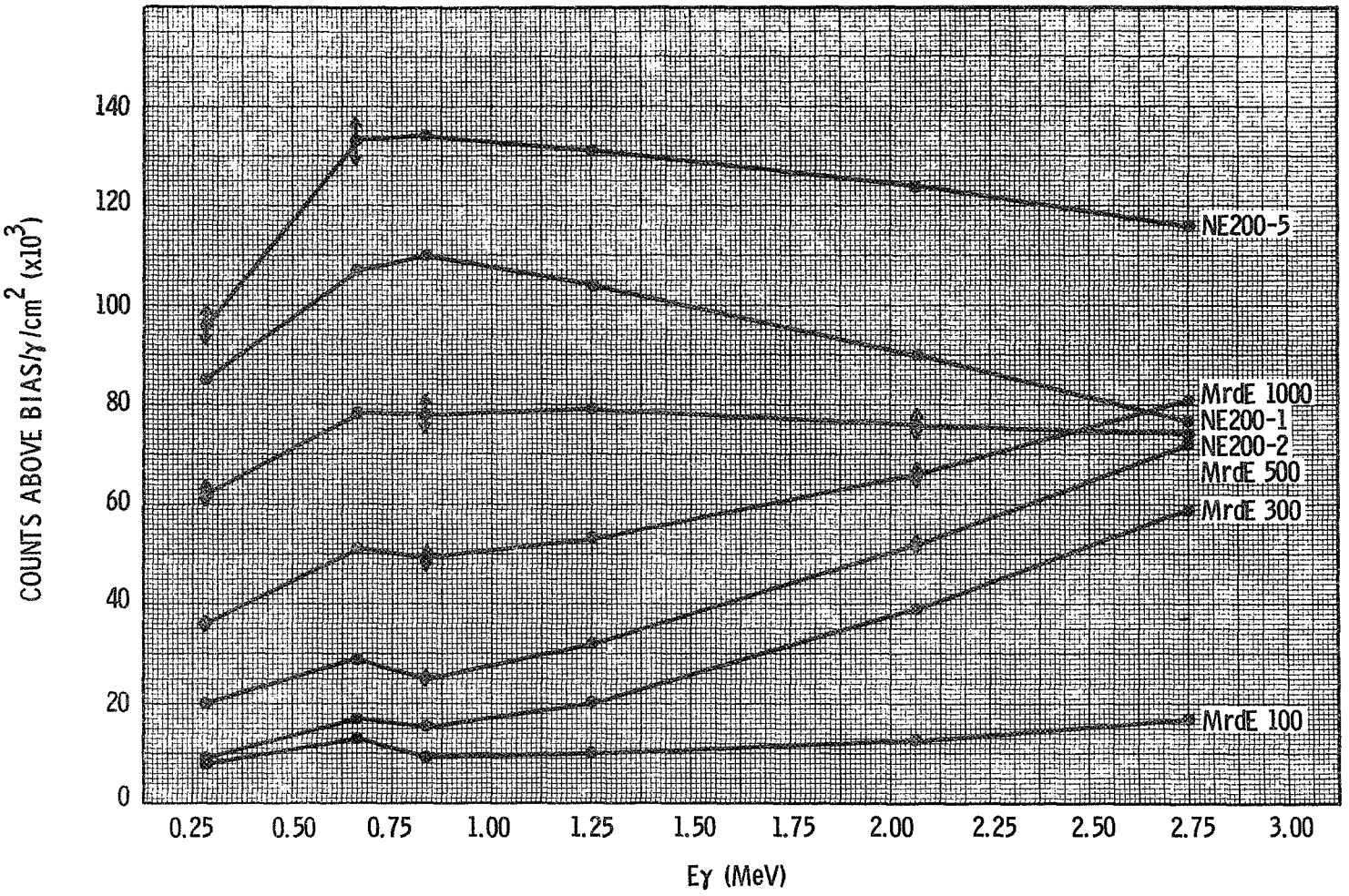

FIGURE 2. DETECTOR RESPONSE VS γENERGY - 75 keV BIAS
(0.090 IN. THICK Al ABSORBER - 2 IN. DIAM. IN CONTACT WITH DET.
EXCEPTION: 0.220 IN. Al FOR Eγ=2.06, 2.75 MeV)

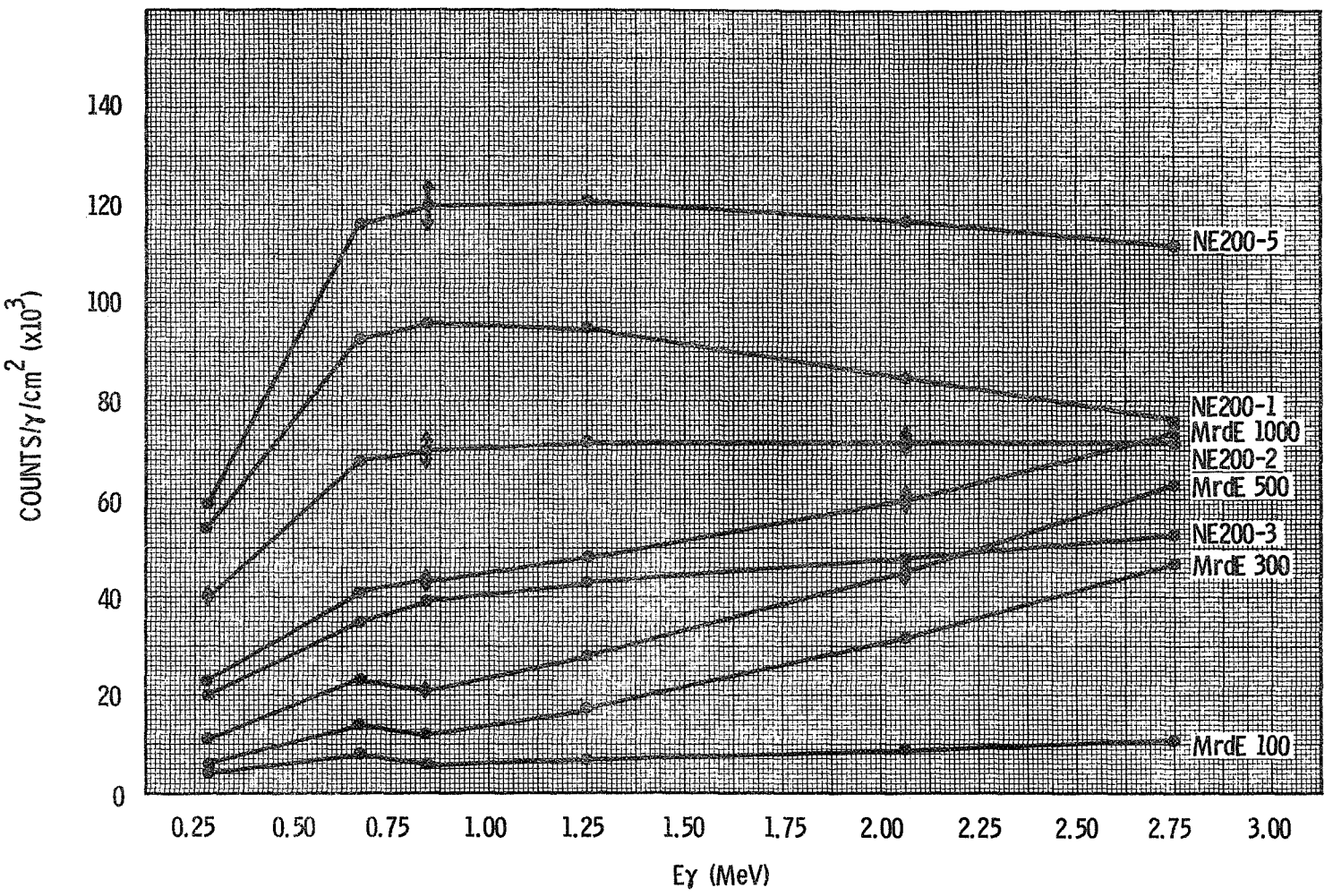

FIGURE 3. DETECTOR RESPONSE VS γENERGY - 100 keV BIAS LEVEL

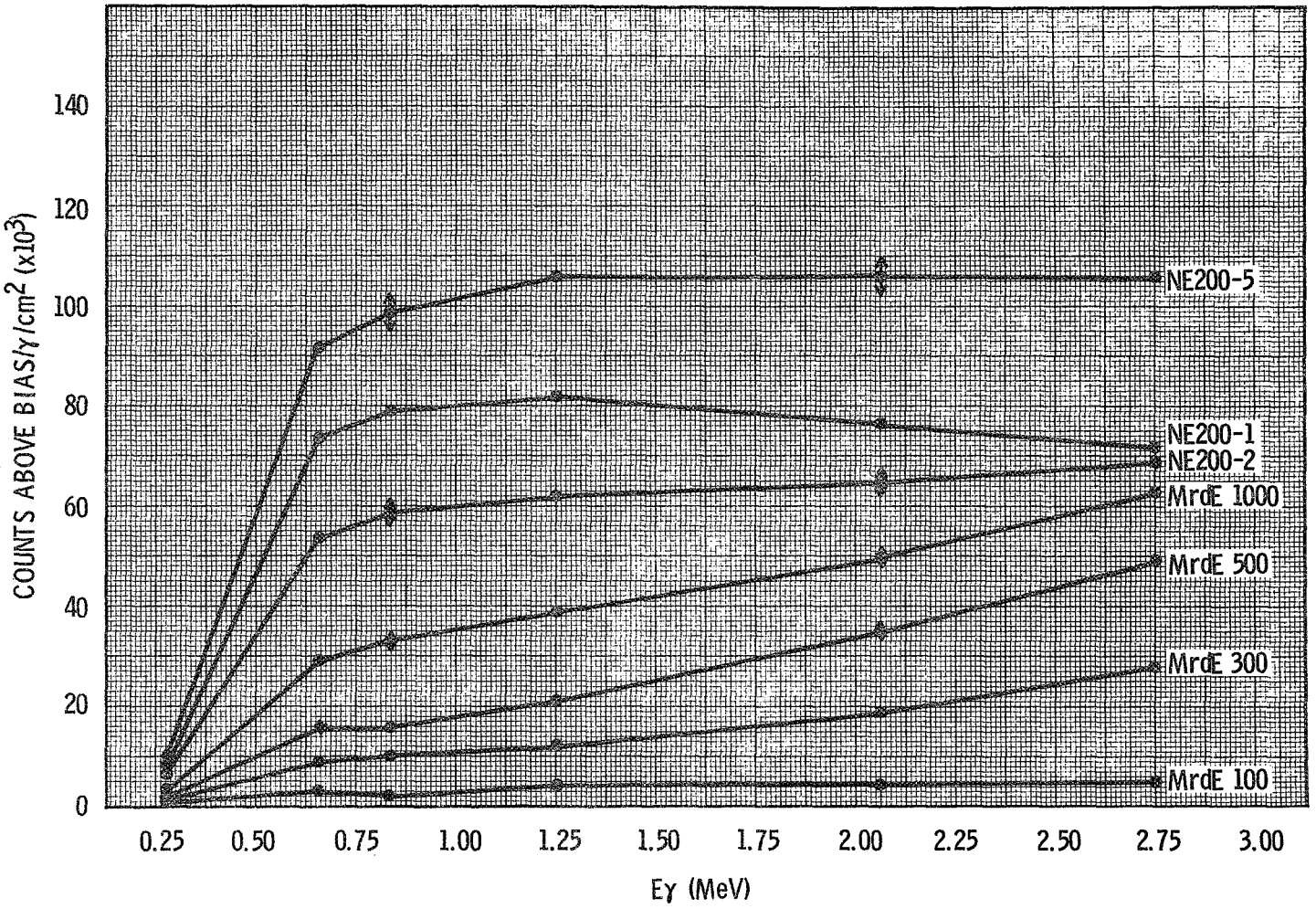

FIGURE 4. DETECTOR RESPONSE VS γENERGY - 150 keV BIAS
(0.090 IN. THICK Al ABSORBER - 2 IN. DIAM. IN CONTACT WITH DET.
EXCEPTION: 0.220 IN. Al FOR Eγ=2.06, 2.75 MeV)

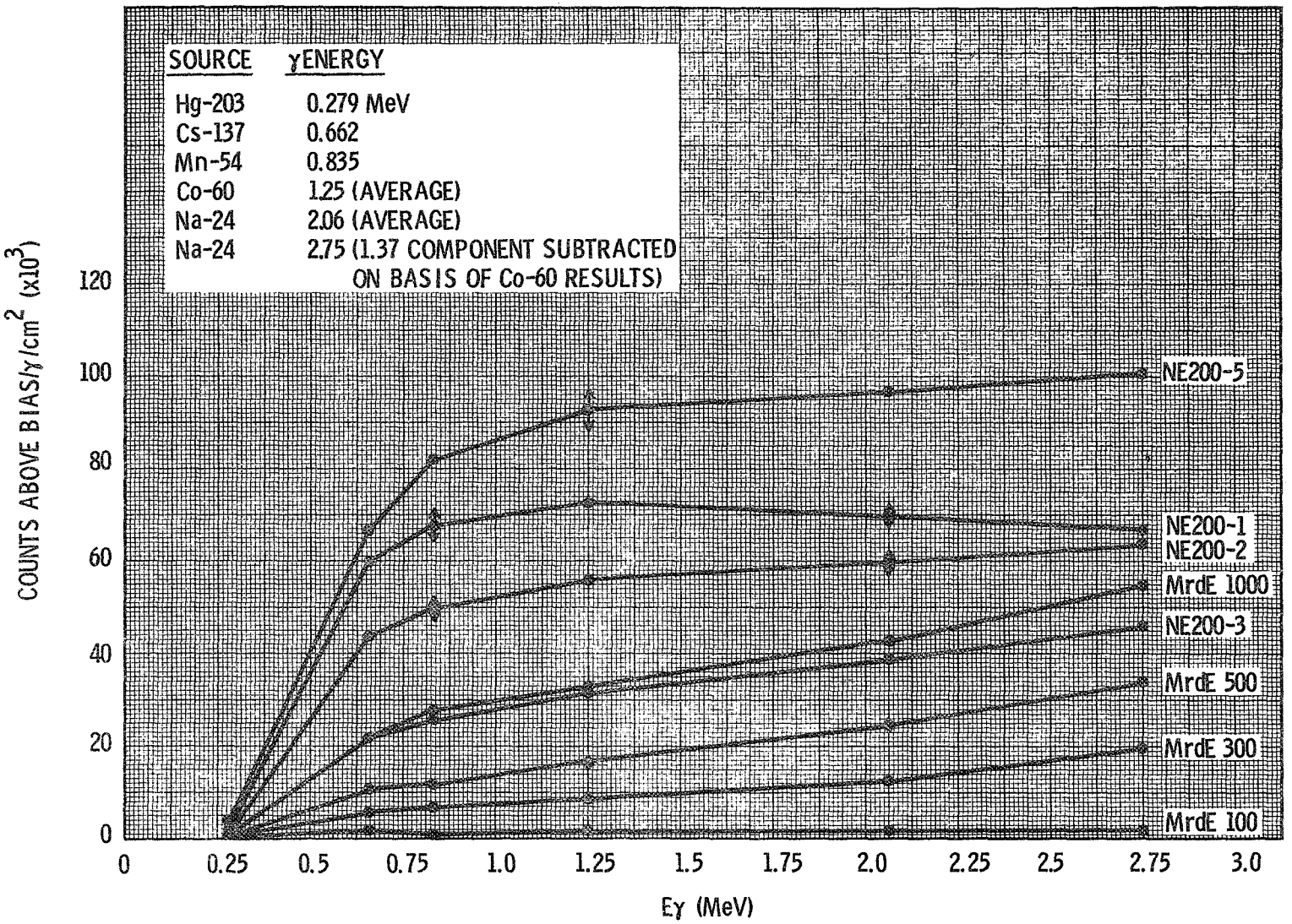

FIGURE 5. DETECTOR RESPONSE VS γENERGY - 200 keV BIAS
(0.90 IN. THICK Al ABSORBER - 2 IN. DIAM. IN CONTACT WITH DET.
EXCEPTION: 0.220 IN. Al FOR Eγ=2.06, 2.75 MeV)

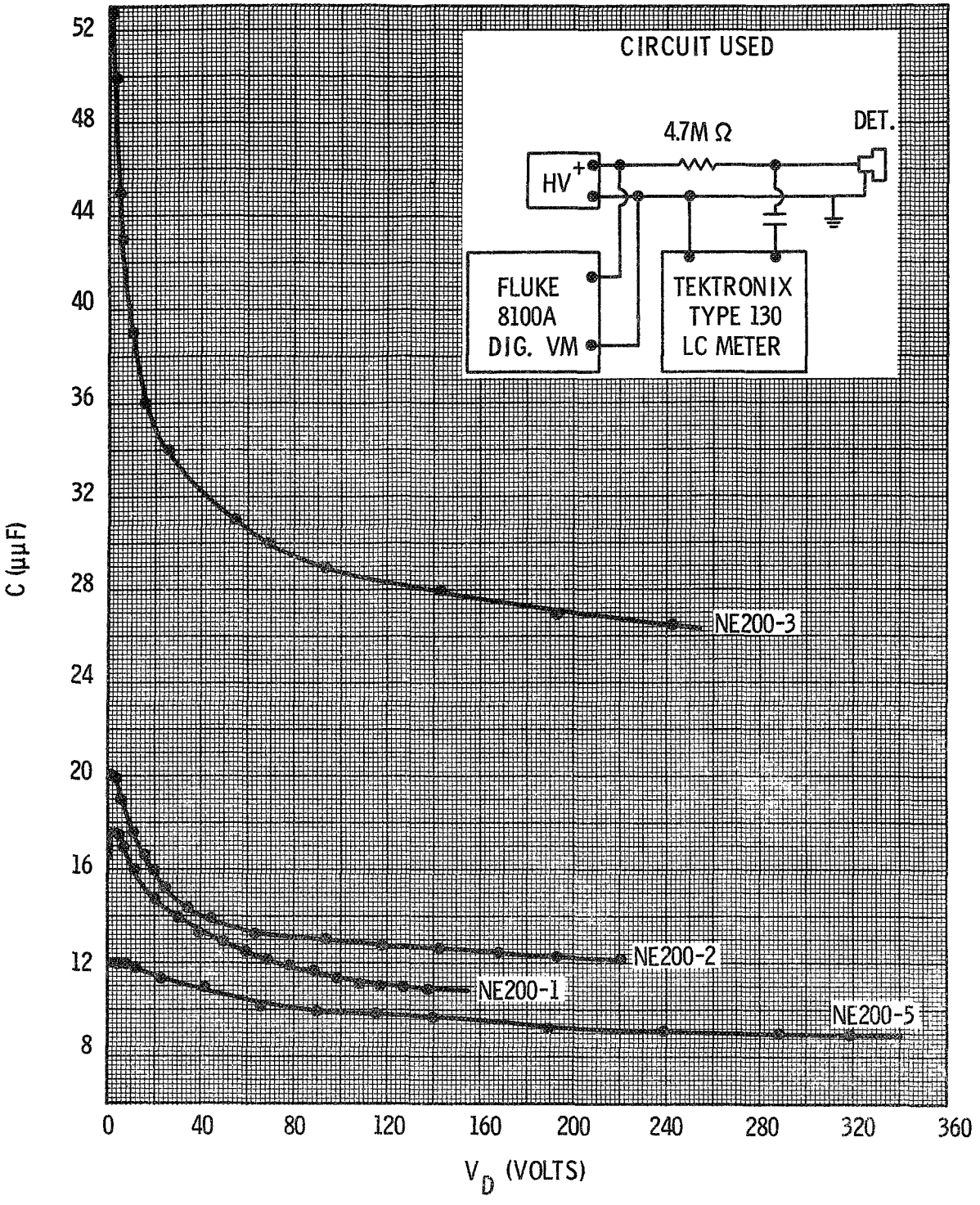

FIGURE 6. Li DRIFTED Si DETECTORS
CAPACITANCE VS BIAS VOLTAGE

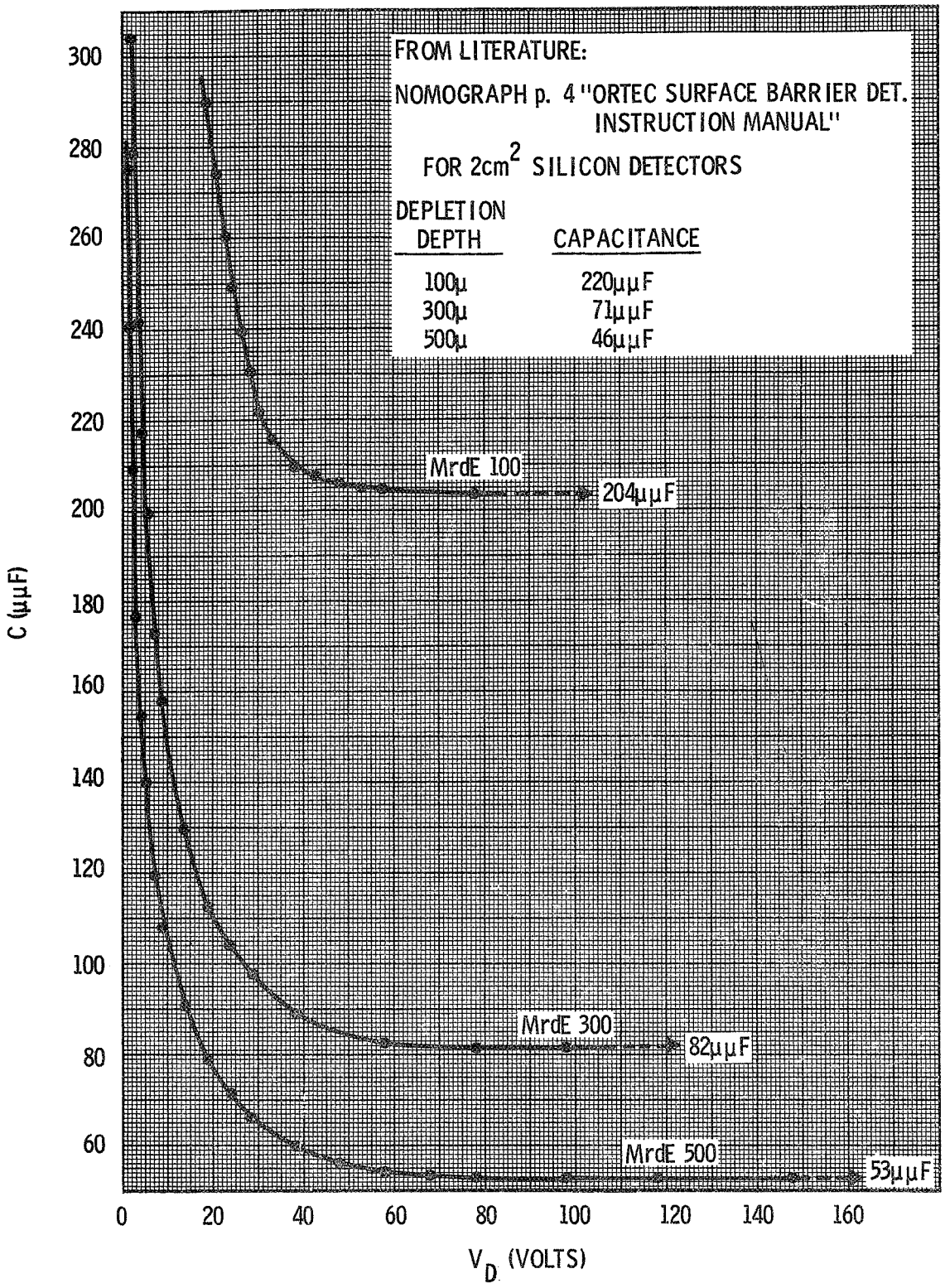

FIGURE 7. SURFACE BARRIER DETECTORS CAPACITANCE VS BIAS VOLTAGE

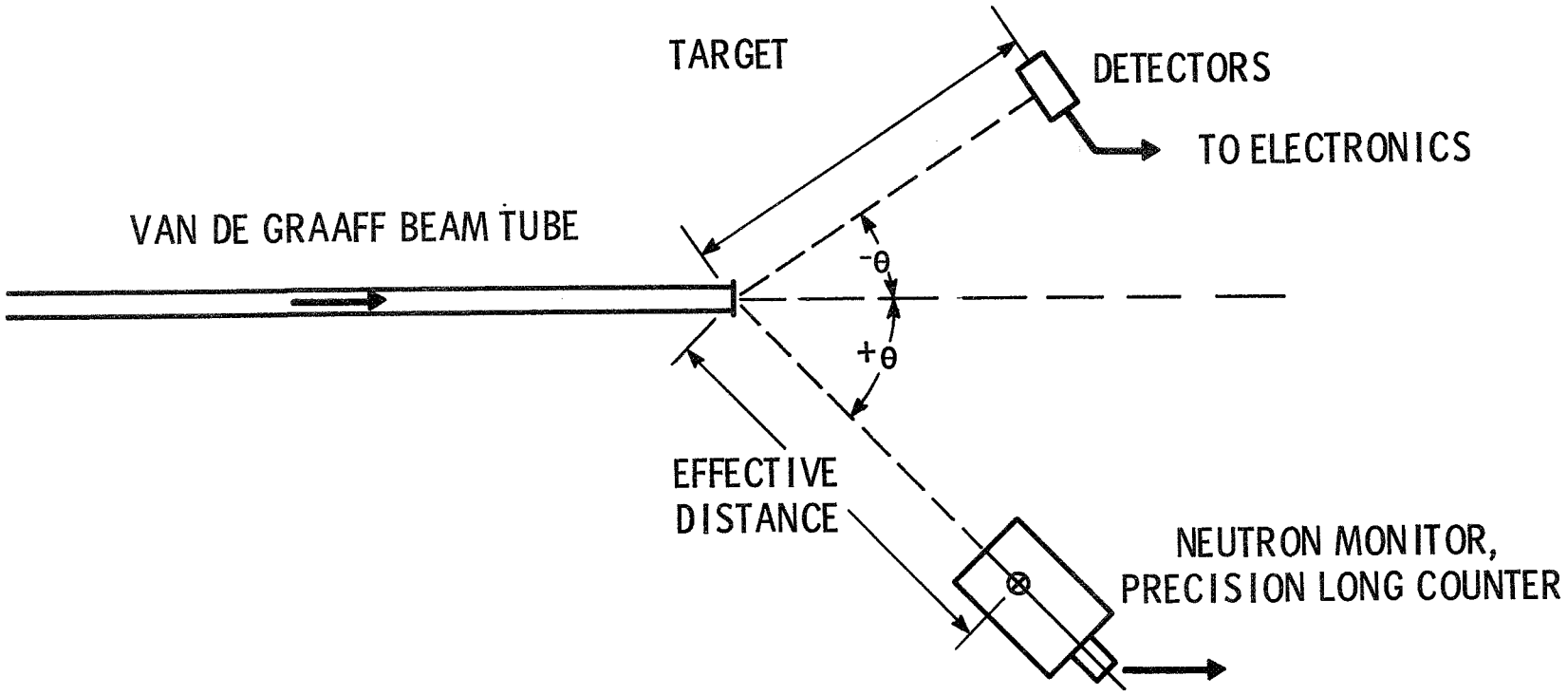
TARGET
DETECTORS
TO ELECTRONICS
VAN DE GRAAFF BEAM TUBE
-θ
+θ
EFFECTIVE
DISTANCE
NEUTRON MONITOR,
PRECISION LONG COUNTER

FIGURE 8.

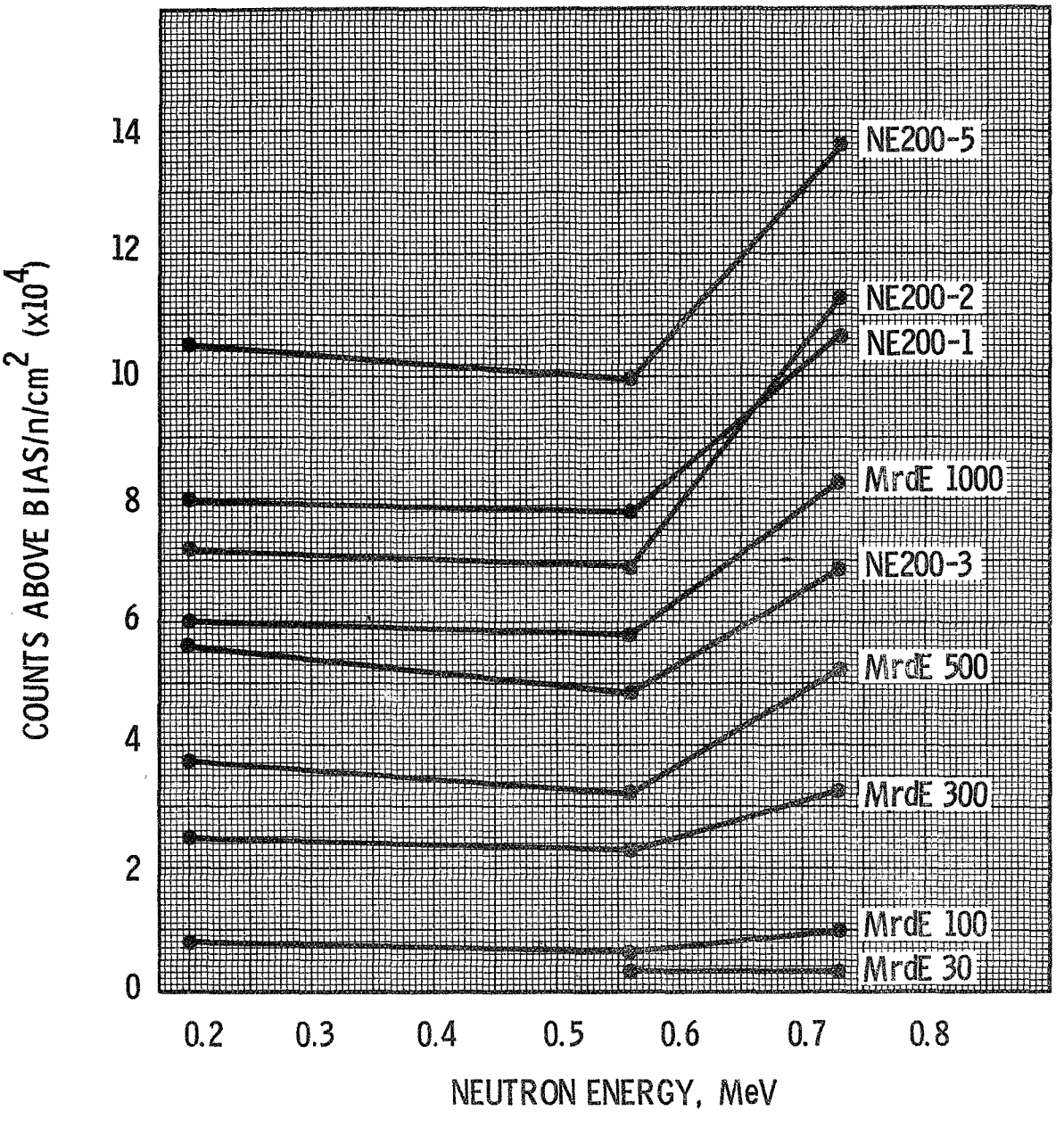

FIGURE 9. DETECTOR RESPONSE VS NEUTRON ENERGY
75 keV BIAS
BACKGROUND SUBTRACTED ON BASIS
OF INVERSE SQUARE RUNS

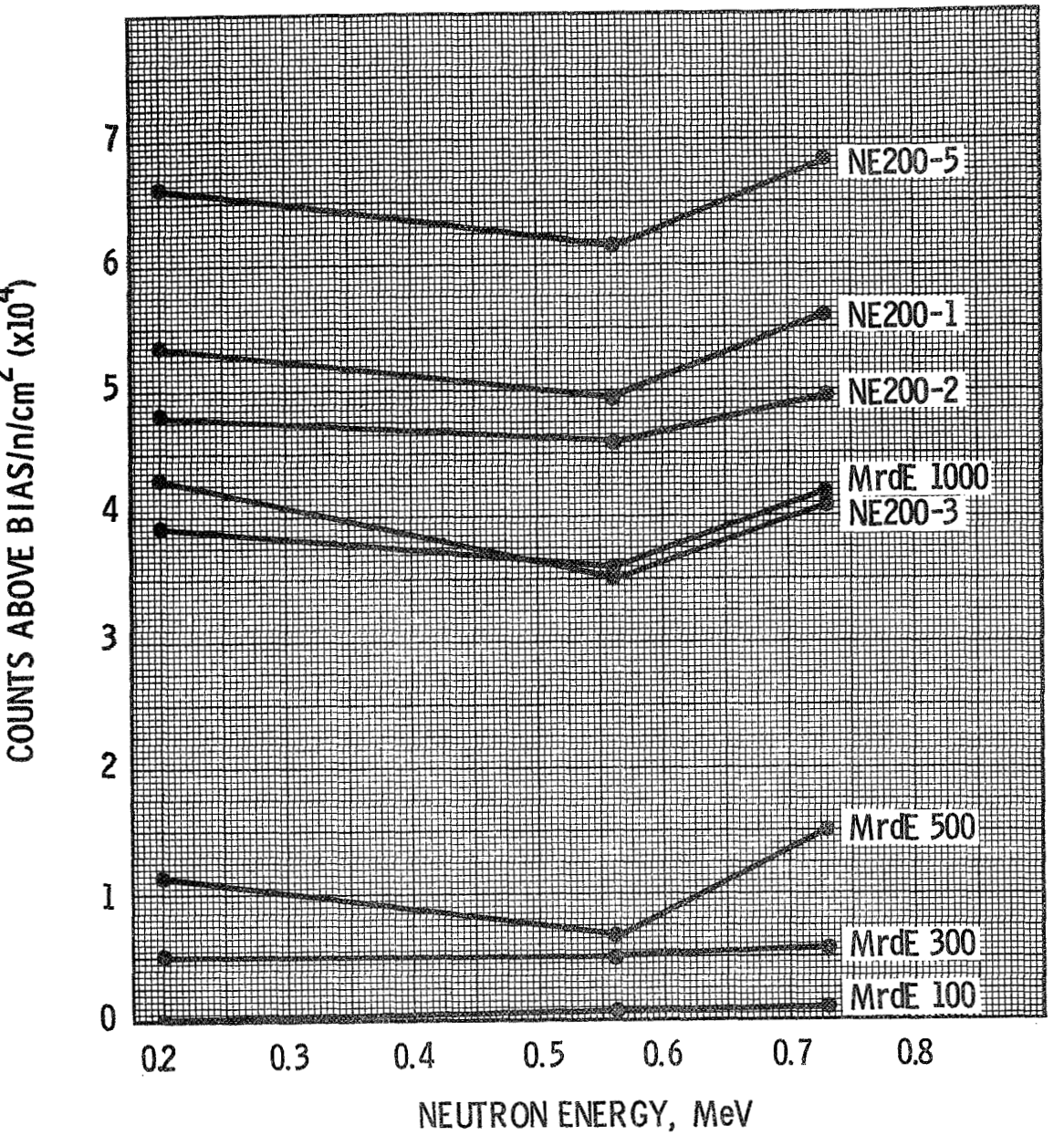

FIGURE 10. DETECTOR RESPONSE VS NEUTRON ENERGY
200 keV BIAS
BACKGROUND SUBTRACTED ON BASIS
OF INVERSE SQUARE RUNS

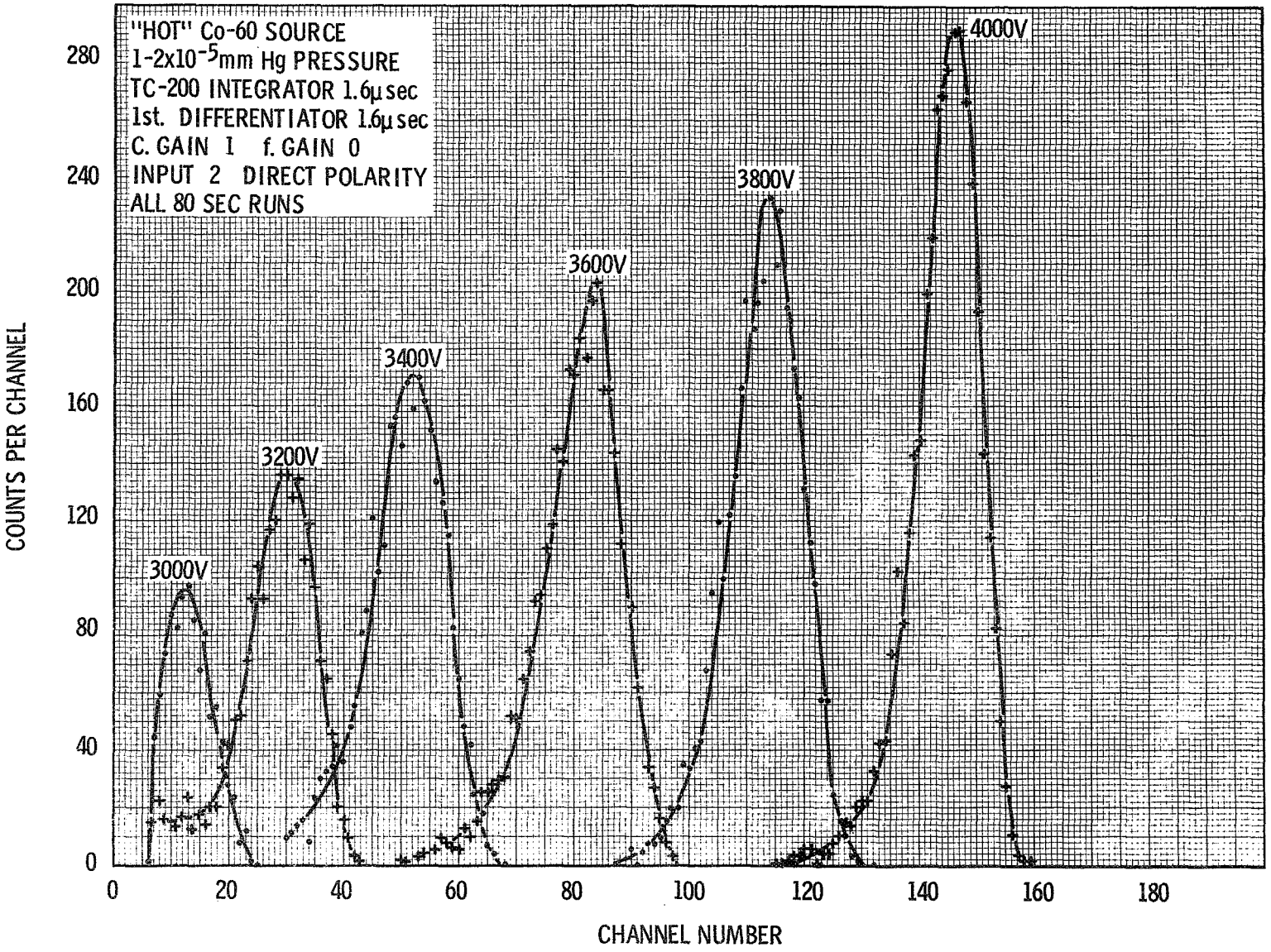

FIGURE 11. CHANNELTRON RESPONSE

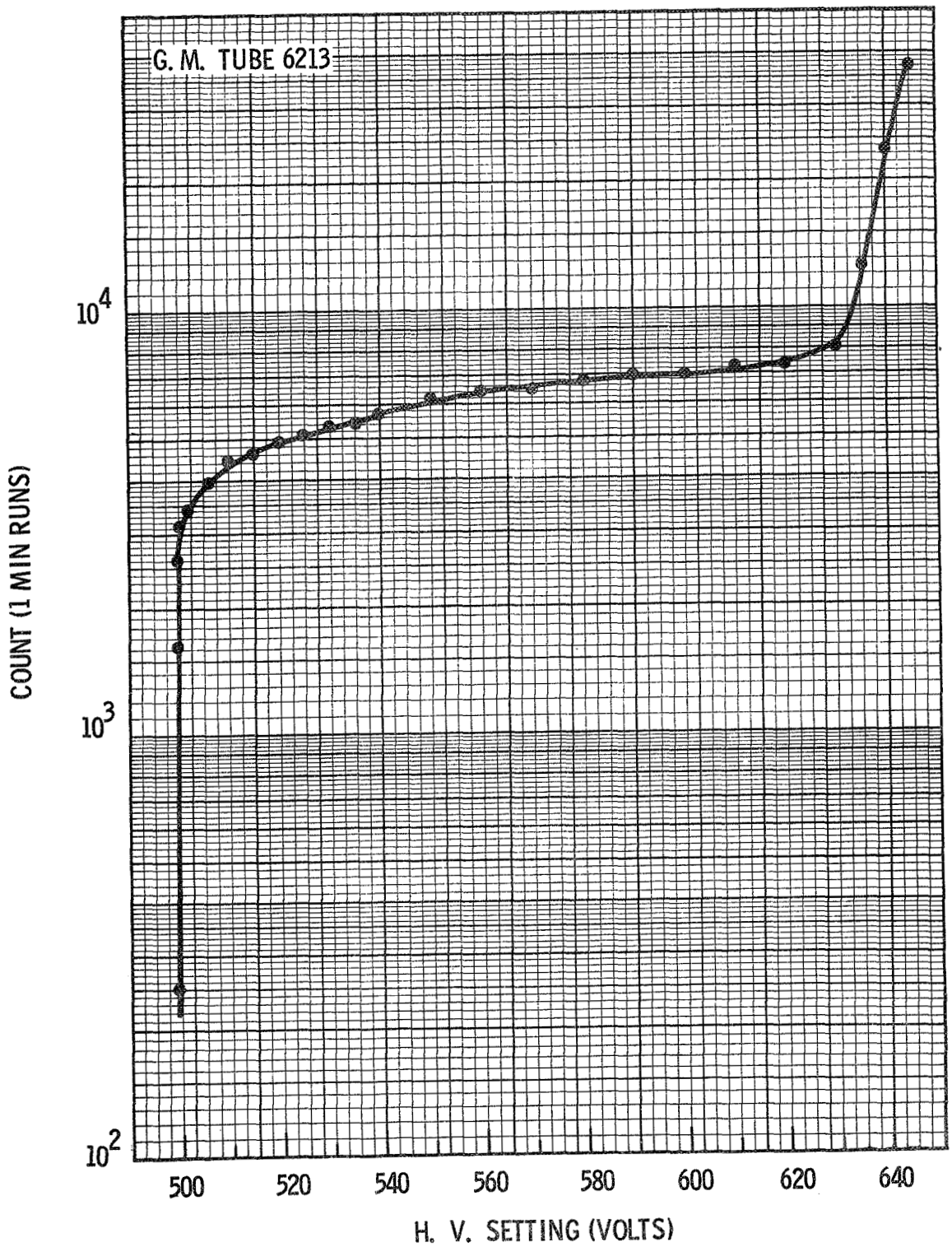

FIGURE 12. PLATEAU DETERMINATION - COUNT RATE VS VOLTAGE

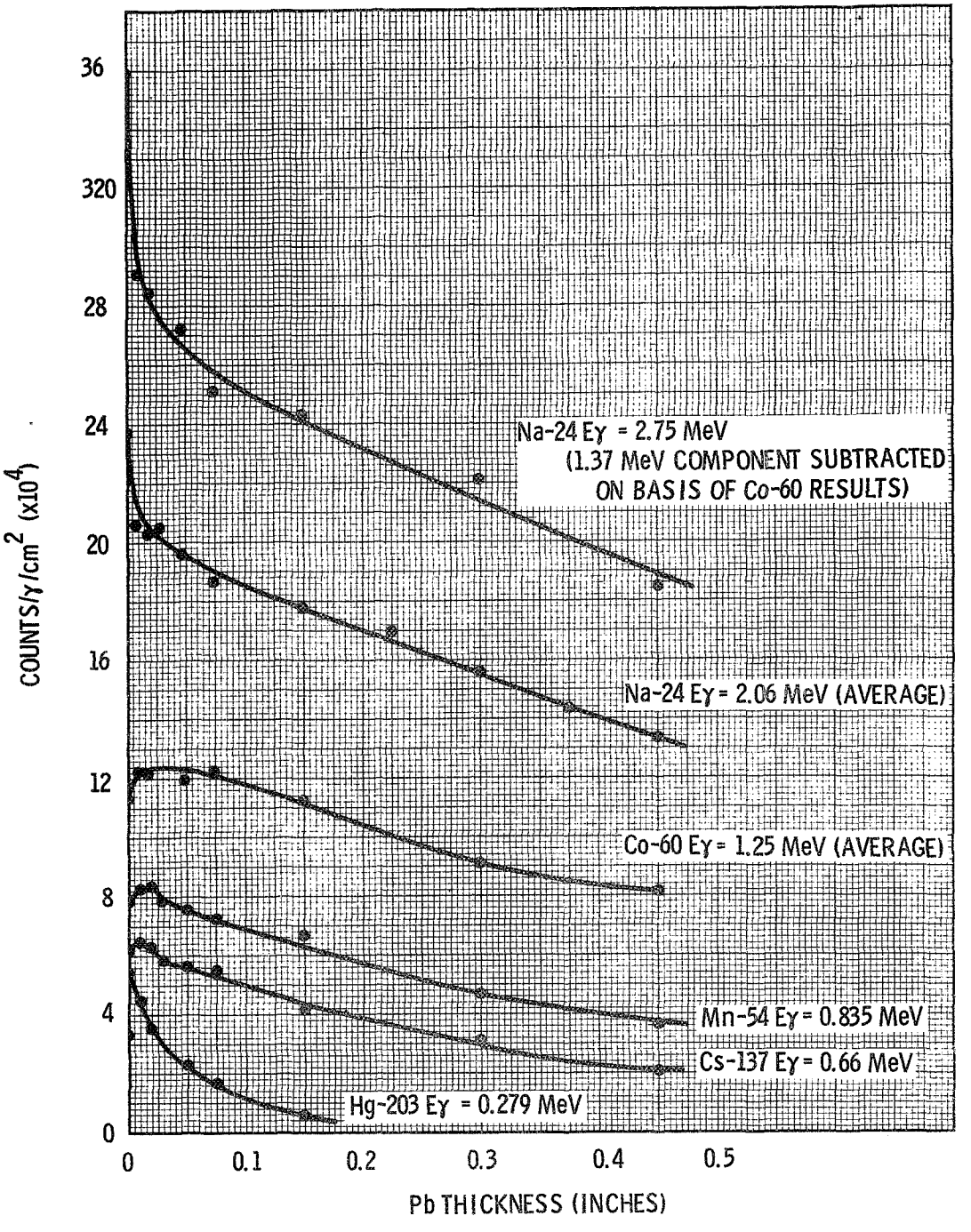

FIGURE 13. GEIGER TUBE 6213 γ RESPONSE VS SHIELD THICKNESS
TUBE OPERATED AT 550 V
CYLINDRICAL Pb SHIELDS 2 IN. LONG
SIDE INCIDENCE OF γ RAYS
CIRCULAR, 0.090 IN. THICK Al ABSORBER OVER
SOURCES - 0.220 IN. THICK OVER Na-24 SOURCE

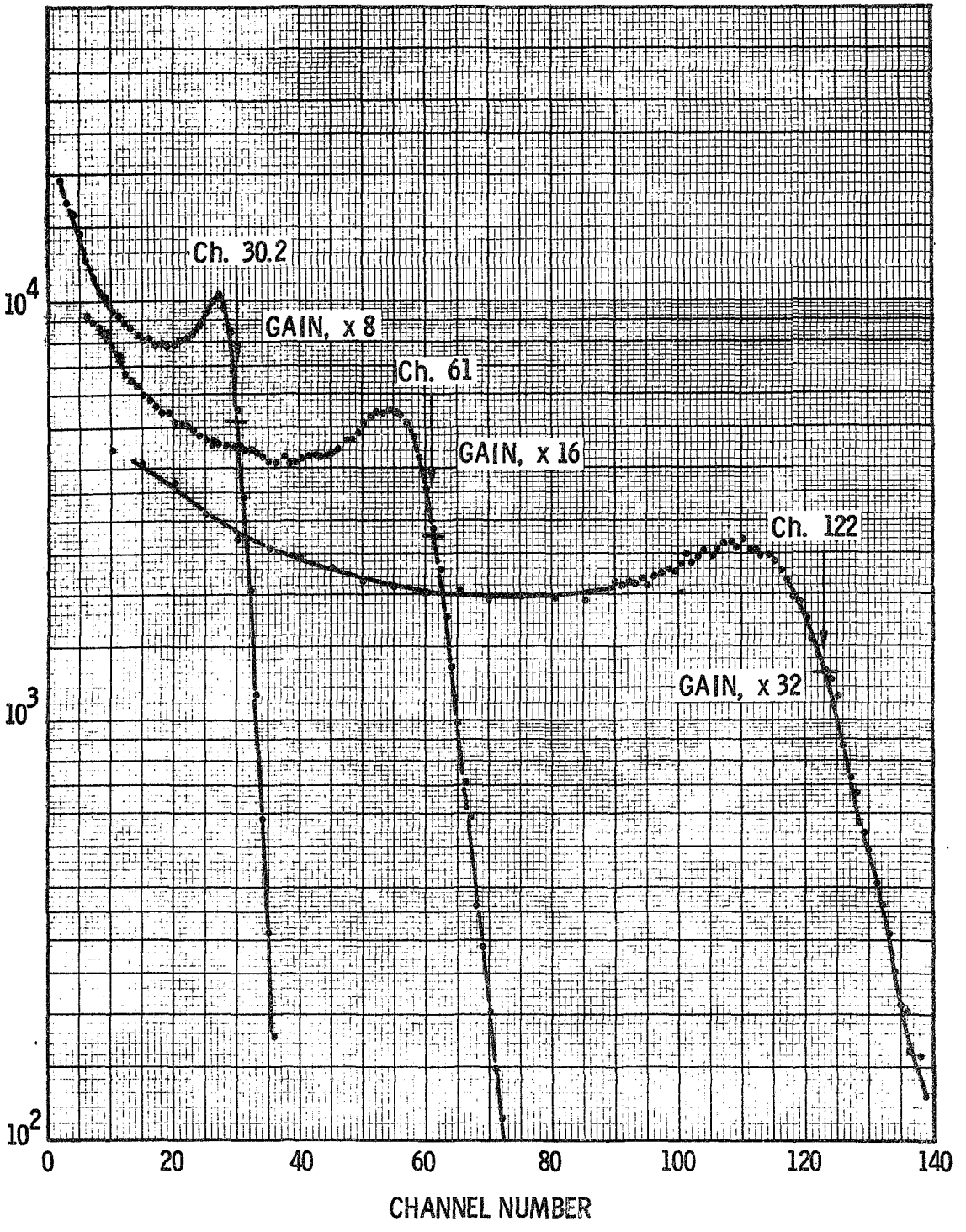

FIGURE 14. Cs-137 SPECTRA FOR 2 IN. DIAMETER SCINTILLATOR
E_γ = 661.6 MeV ,
E_C = 477.3 MeV

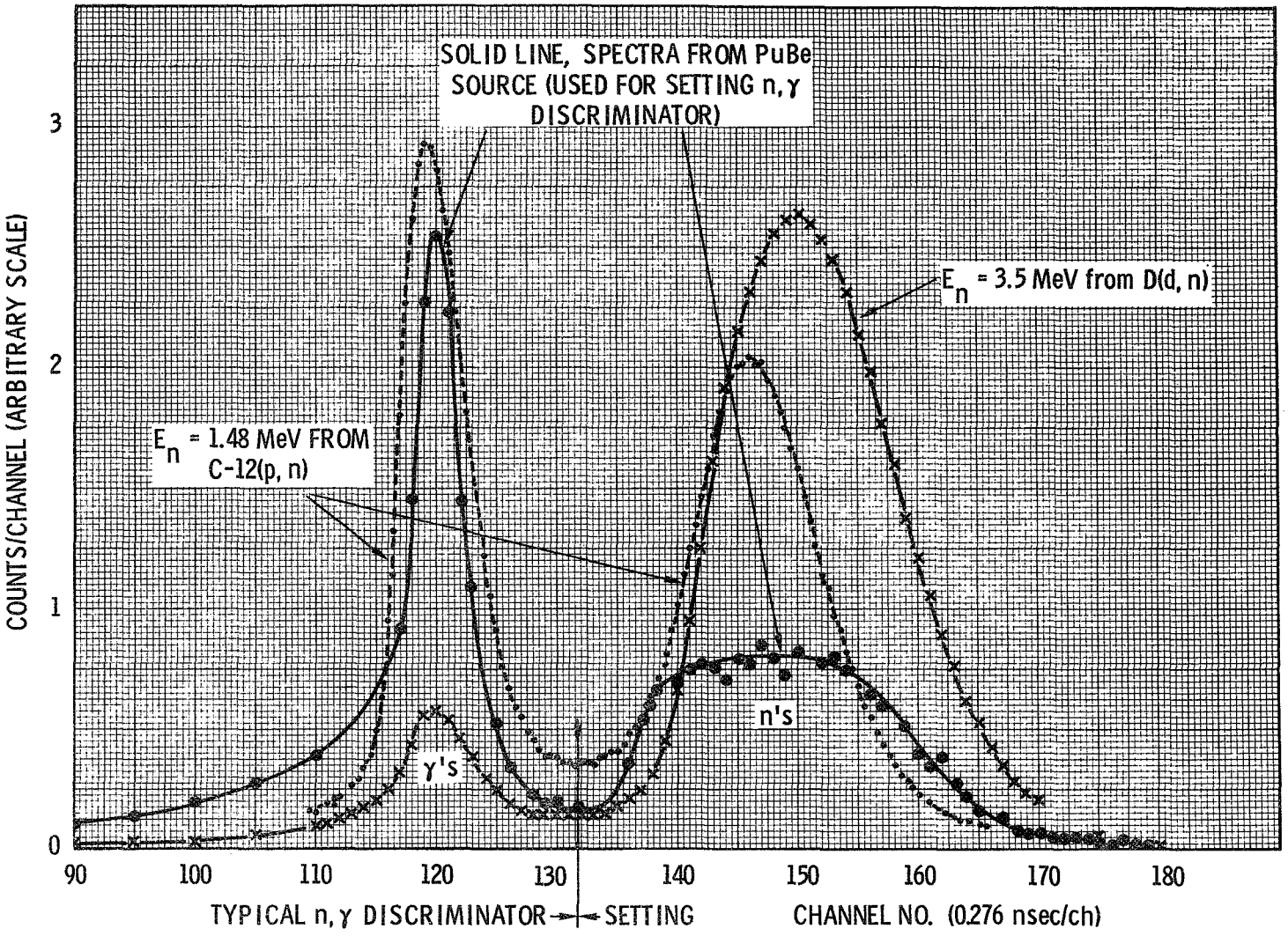

FIGURE 15. REPRESENTATIVE n,γ TIMING SPECTRA

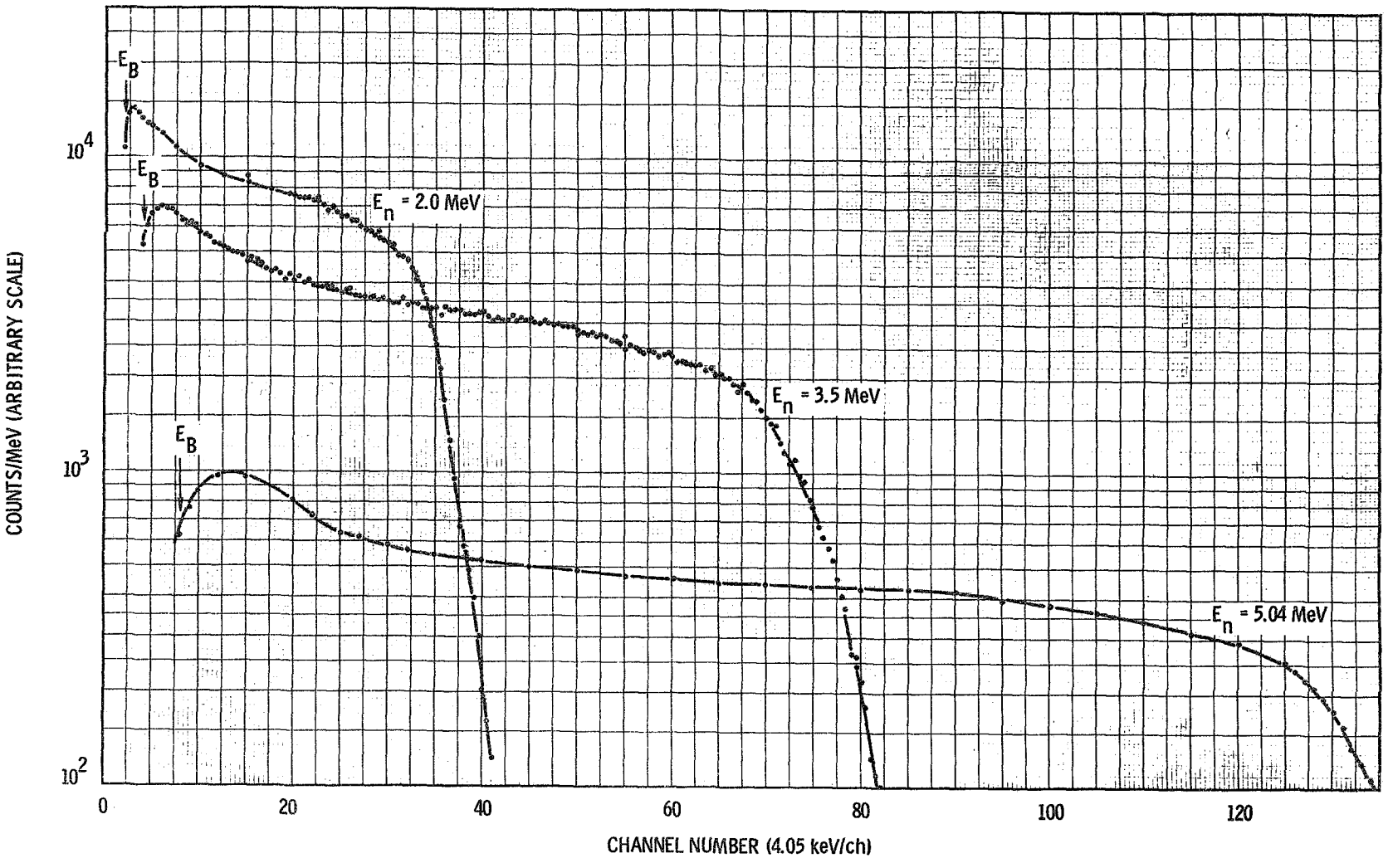

FIGURE 16. SCINTILLATOR PULSE HEIGHT SPECTRA FOR MONOENERGETIC NEUTRONS

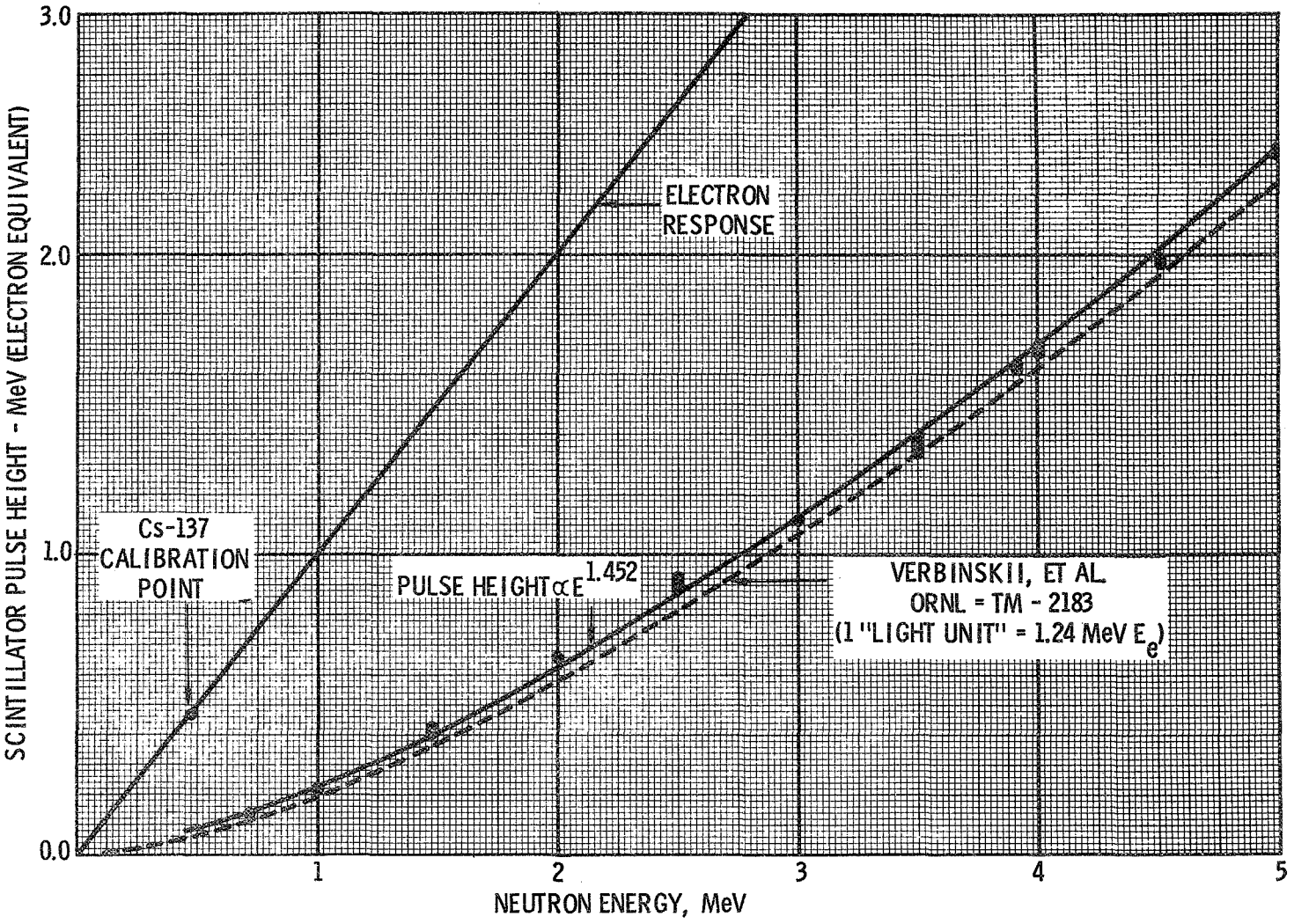

FIGURE 17. PEAK SCINTILLATOR LIGHT OUTPUT VS NEUTRON ENERGY

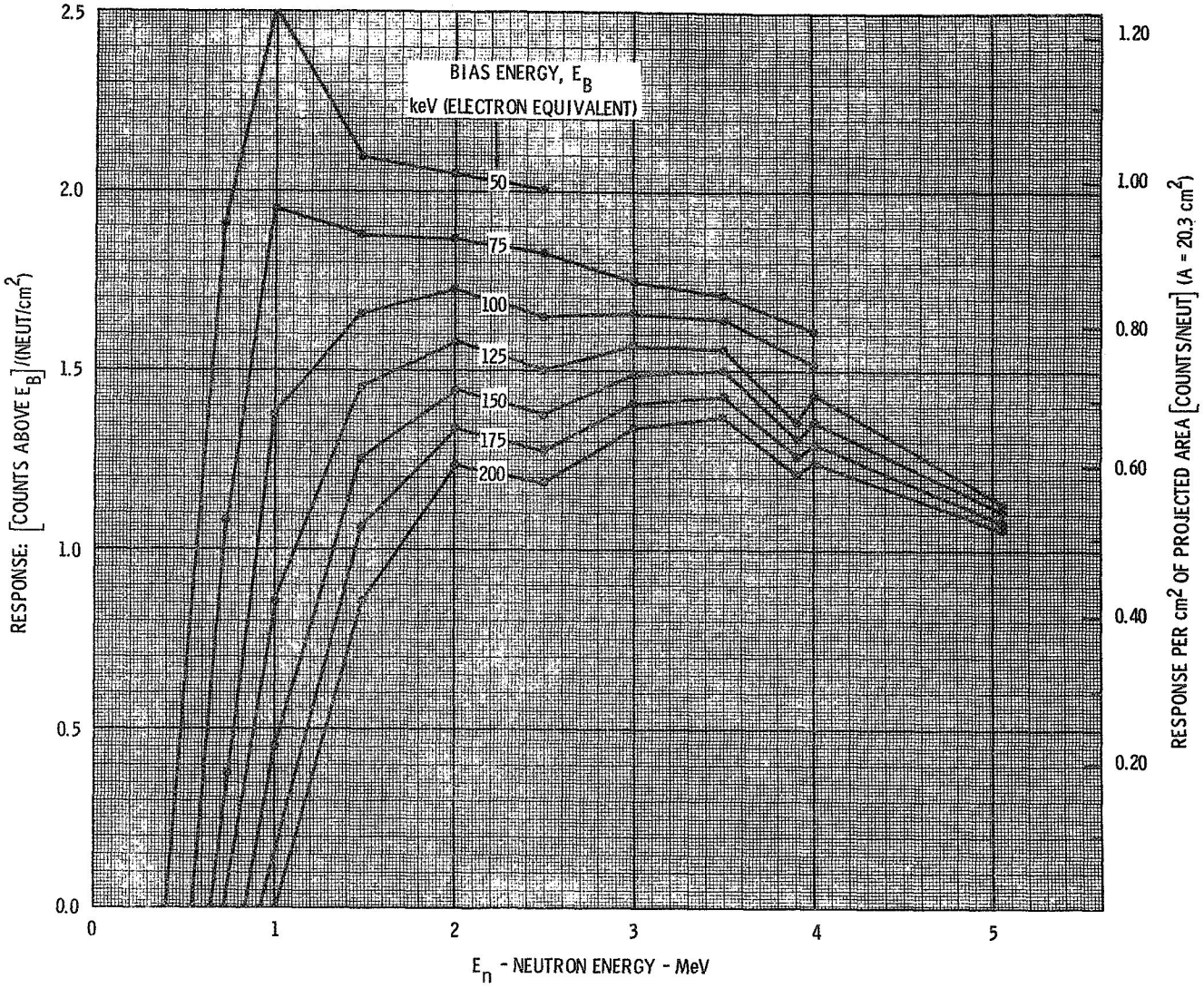

FIGURE 18. NEUTRON RESPONSE OF SCINTILLATOR NE-213
2 IN. DIAM. x 0.4 IN. THICK (JPL #1)
NORMAL INCIDENCE, ALONG AXIS

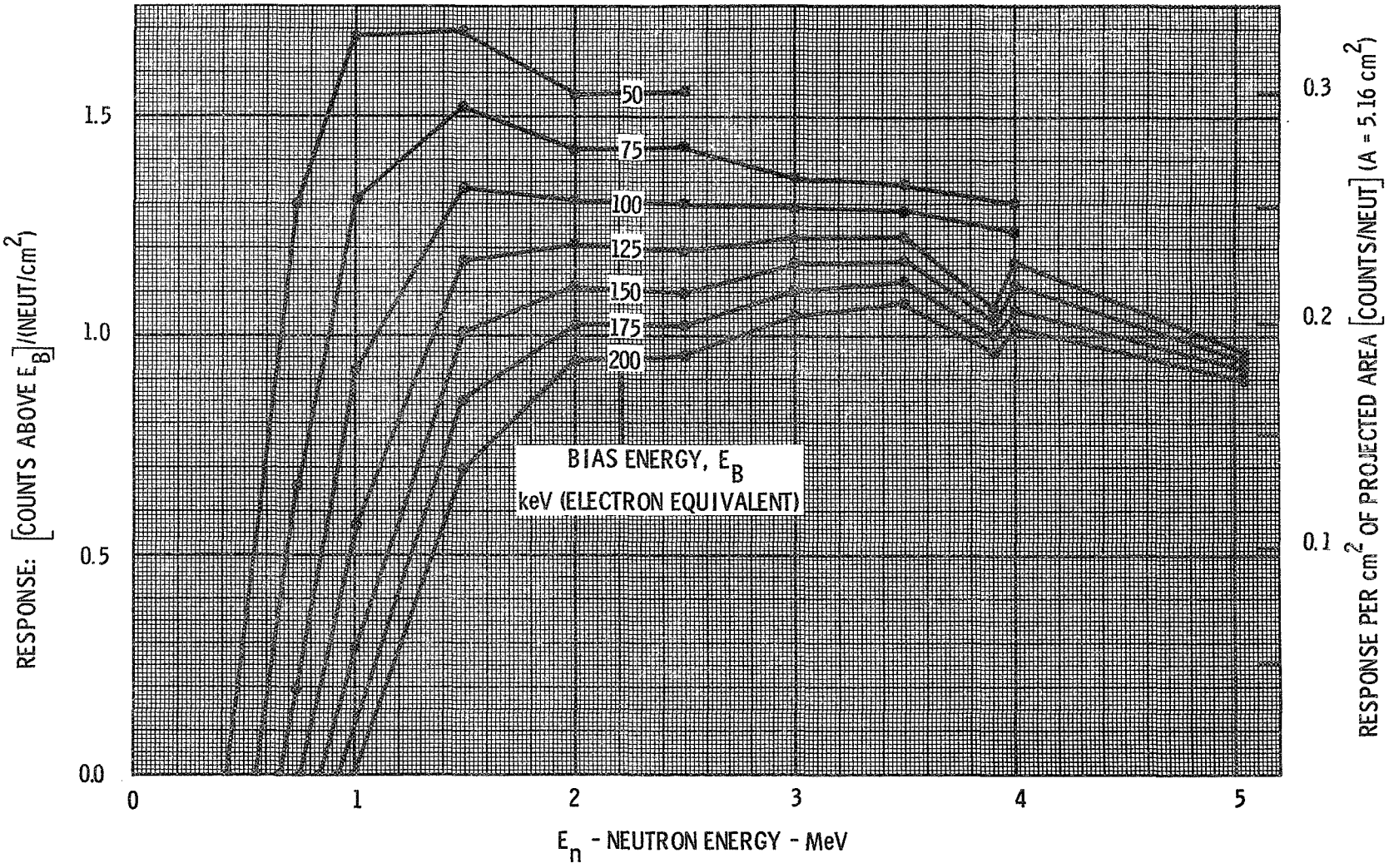

FIGURE 19. NEUTRON RESPONSE OF SCINTILLATOR NE-213
2 IN. DIAM. x 0.4 IN. THICK (JPL #1)
SIDE INCIDENCE, PERPENDICULAR TO AXIS

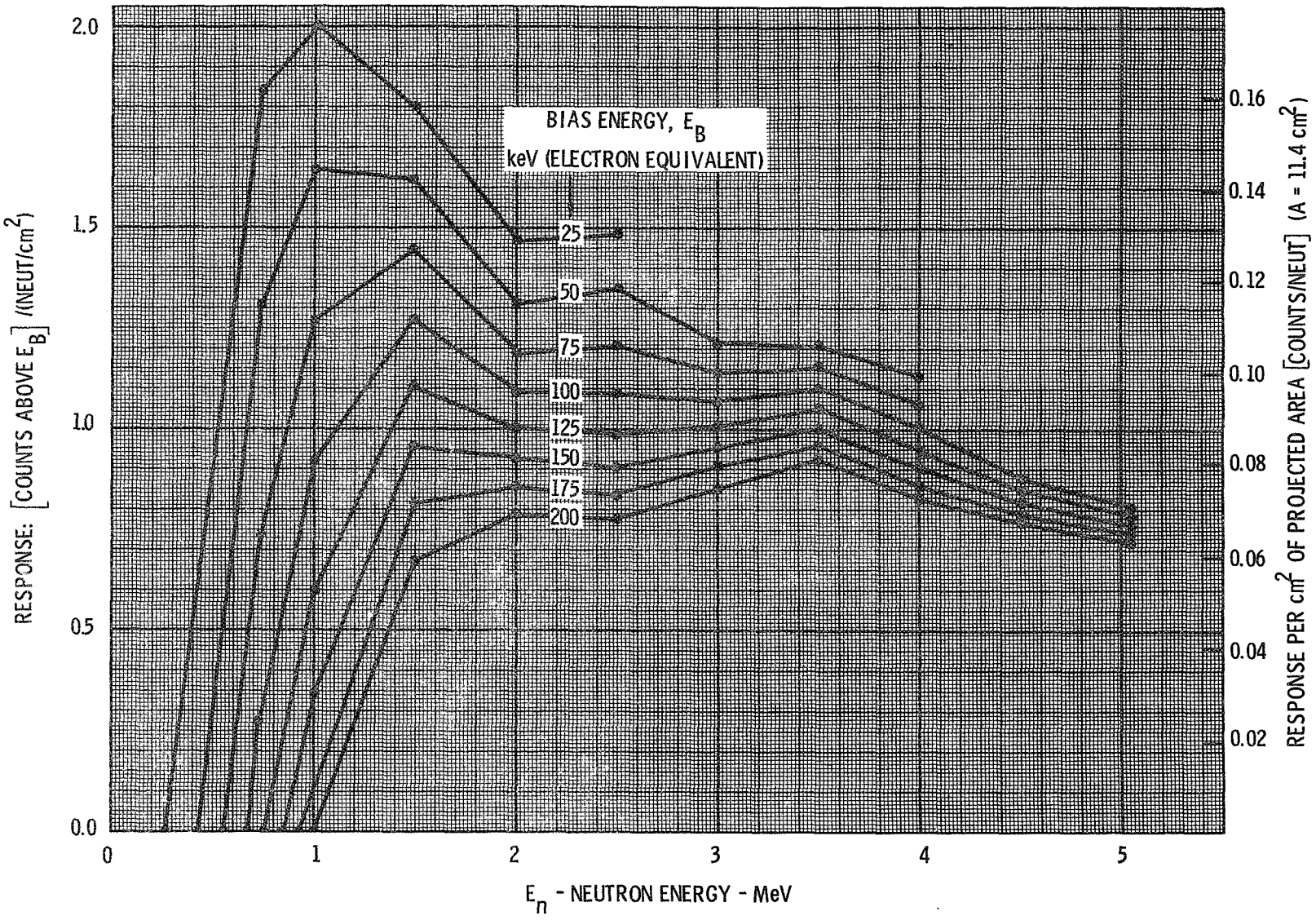

FIGURE 20. NEUTRON RESPONSE OF SCINTILLATOR NE-213
1.5 DIAM. x 0.4 IN. THICK
NORMAL INCIDENCE, ALONG AXIS

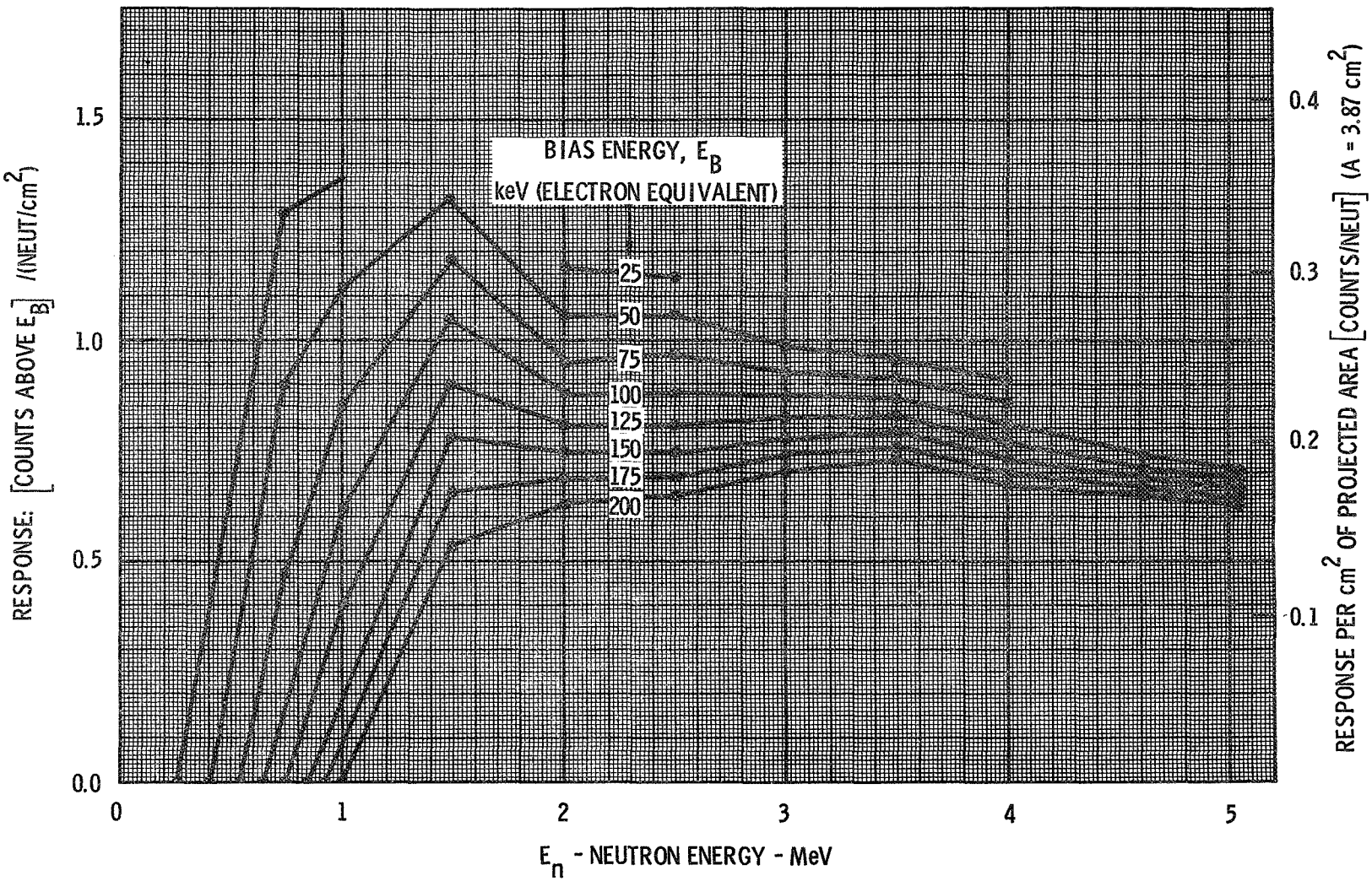

FIGURE 21. NEUTRON RESPONSE OF SCINTILLATOR NE-213
1.5 IN. DIAM. x 0.4 IN. THICK
SIDE INCIDENCE, PERPENDICULAR TO AXIS

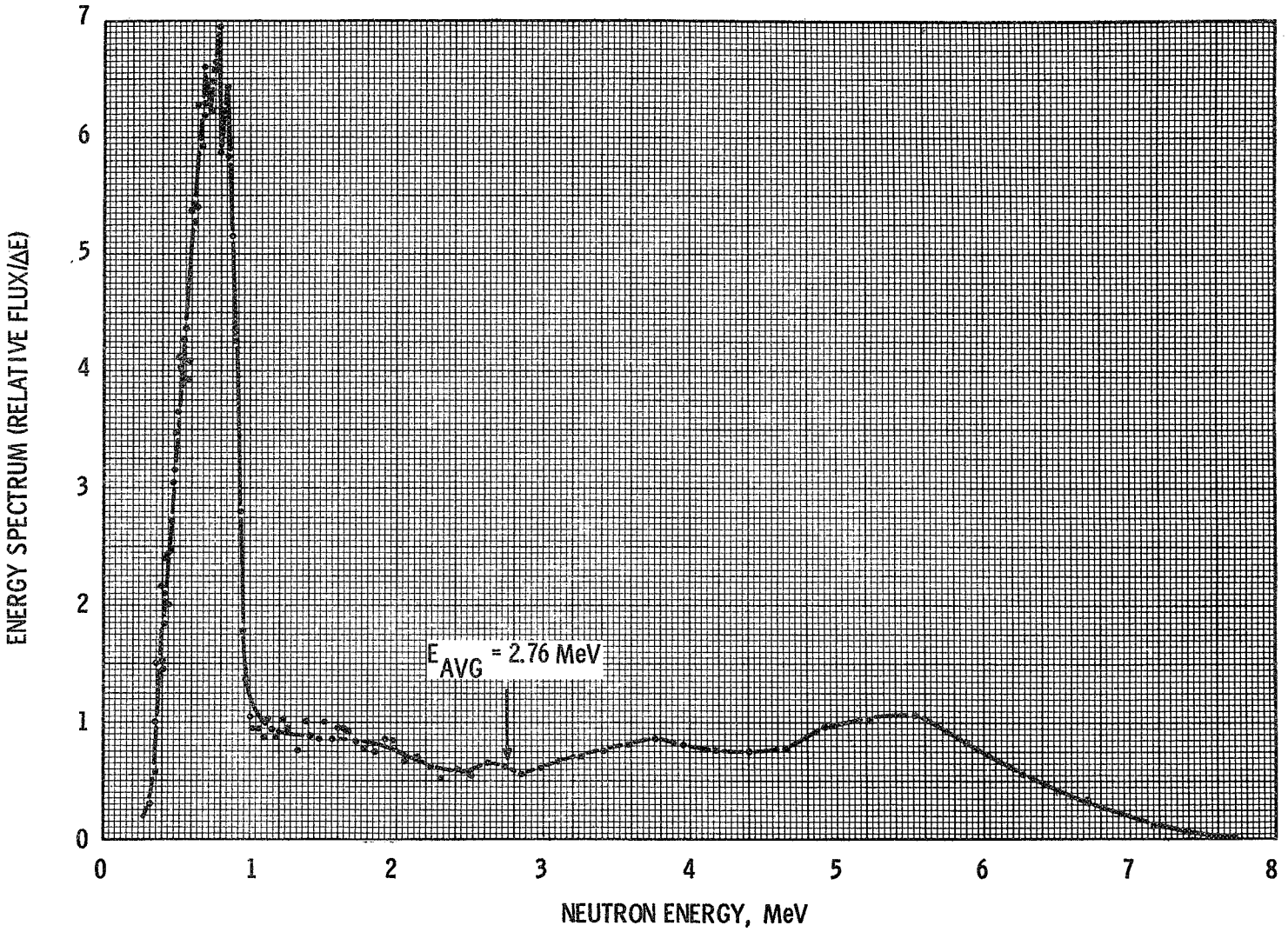

FIGURE 22. NEUTRON ENERGY SPECTRUM - Be(d,n) THICK TARGET
E_d = 1.8 MeV
(CONVERSION FROM T-O-F TO ENERGY SPECTRUM MADE USING JPL CALCULATED RESPONSE ABOVE 10 keV BIAS FOR 1.016 cm THICKNESS.)

APPENDIX

SCINTILLATION NEUTRON SPECTROMETER SYSTEM

BLOCK DIAGRAM

AND

CONTROL SETTINGS

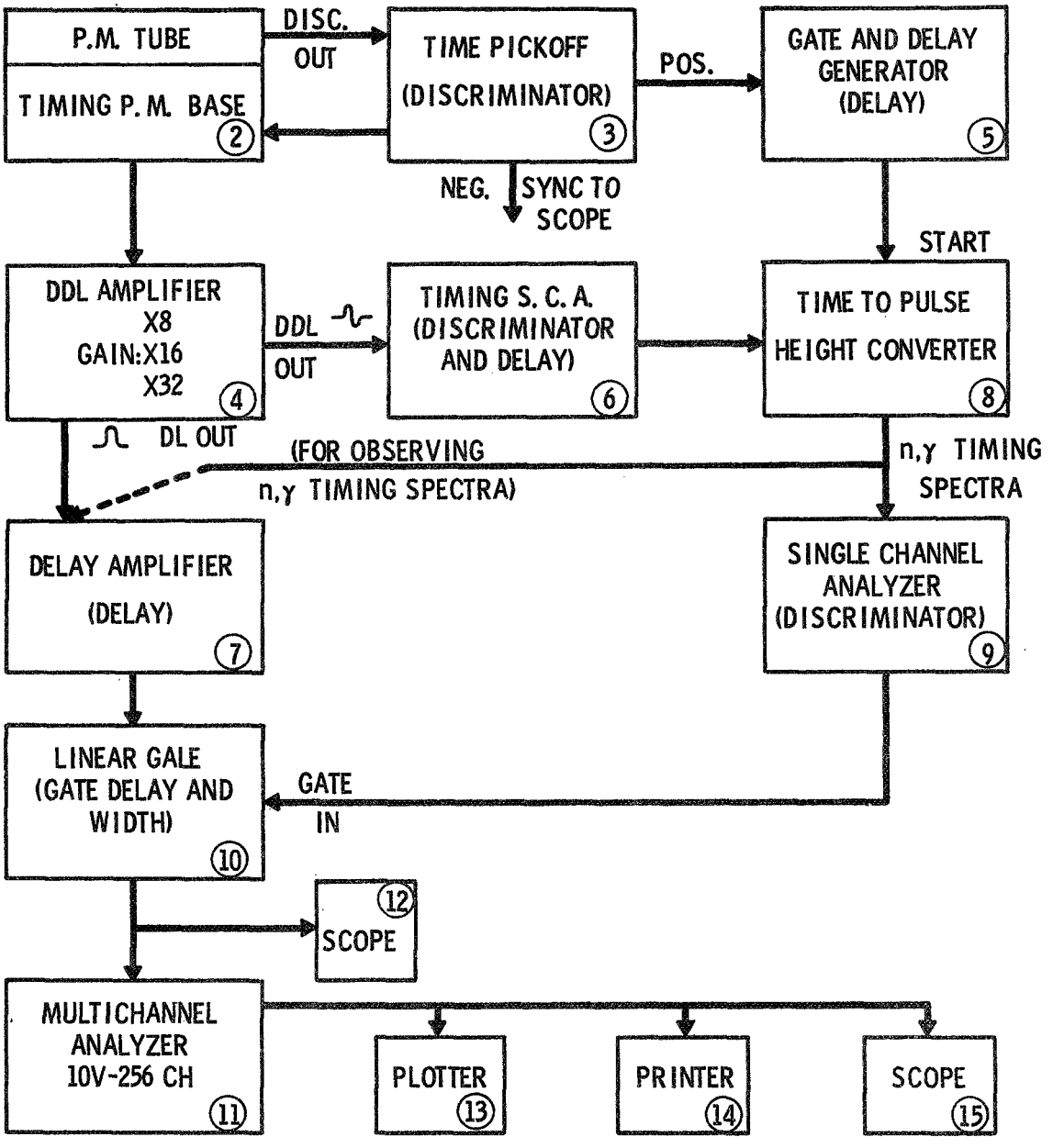

BLOCK DIAGRAM
SCINTILLATION NEUTRON SPECTROMETER (n,γ DISCRIMINATING)

BLOCK DIAGRAM COMPONENTS AND SETTINGS

1. Constant Fraction Timing P.M. Base. ORTEC Model 270. (It must be used with an ORTEC Model 403A Control, 3.)

   Internal Adjustments Only.

2. P.M. High Voltage Supply, 0-3000 V Calibration Standards Corporation, Model 122 B.

   Negative 2050 and 2200 V values were used.

3. Time Pickoff Control

   ORTEC Model 403 A

   a) Disc. Level: 1.0 for nearly all runs.

   b) Output 3 (pos.) used for start via (5).

   c) Output 1 or 2 (neg) used for oscilloscope sync.

4. DDL Amplifier

   Canberra Industries Model 1411

   a) Coarse Gain: Various, x 8, x 16 and x 32 used.

   b) Time Gain: Always min (CCW), or 4.

   c)Input Mode: Pos., 1/10.

   d) DDL Output to Timing SCA (6).

   e) DL Output to P.H. Analyzer via (7) and (10).

5. Gate and Delay Generator

   ORTEC Model 416

   a) Delay Range: 1.0 - 11 us.

   b) Delay Pat: 2.00

   c) Delayed Gate: Width 0.4 us.

d) Delay Gate: Amplitude 4V.

e) Delayed Gate: Neg. output to start input of (8).

6. Timing Single-Channel Analyzer

ORTEC Model 420

a) Disc. "E": Varied, used at 0.20 and 0.30.

b) Disc. ΔE: Not relavent.

c) Mode: Integral, Bipolar

d) Walk: Adjusted for best resolution of n,γ timing spectra from time-P.H. Conv. (8).

e) Neg. output to stop input of (8).

7. Delay Amplifier

ORTEC Model 427

a) Delay switches set for total of 3.5 us.

8. Time-to-Pulse Height Converter

ORTEC Model 437 A

a) Range: 0.1 us.

b) Multiplier: x 1

c c) Amplitude: 10 V

d) Output Delay: Min, ccs, 0.5 ux.

e) Strobe: Internal, gate anticoincidence

f) output, 93 ohm: to timing SCA (9)

g) Output, 1 ohm: to delay amp (7) (in place of DDL Amp. DL output) when checking n,γ timing discrimination point.

9. Timing Single-Channel Analyzer

Canberra Industries Model 1436

a) Window: Not relevant.

b) Base Line: Primary adjustment for n,γ discrimination. Settings varied between 2.5 and 3.5 and can be critical ($\pm$ 0.02).

c) Delay: 0.0.

d) Mode: LE and SCA.

e) Output: Pos. to gate (10).

10. Linear Gate

Canberra Industries Model 1451

a) Gate Mode: On for n,γ discrimination

Gate Mode: Off cor no n,γ discrimination and for examining n,γ timing spectra from T-PH Conv. (8,g).

b) Gate Width: 3.0

c) Gate Delay: 0.95

(Gate width and delay adjusted to accept arrival time of DL pulse from DDL Amp (4). Other delay adjustment possible in Delay Amp. (7).

11. Multichannel Analyzer

Nuclear Data ND2200, 1024 Channel

a) Usually operated as four 256 channel groups.

b) Input: + 10 V, Delayed ADC and Discrim.

c) Conversion Gain: 256.

d) Linear Gate Closed. Lower disc 1.3, at about channel one or two.

11. (Cont'd)

    e) Upper Disc: 10.0.

    f) Monitor Oscilloscope: Tektronix Type RM 503.

12. Oscilloscope Tektronix 555 with Type L Plug in.

    a) Sweep trigger: Ext. from P.M. Time pick off (3).

13. Plotter, Houston Ommigraphic Model 6550.

14. Printer, Monroe Data/Log.